İSTANBUL TECHNICAL UNIVERSITY ★ INSTITUTE OF SCIENCE AND TECHNOLOGY

VIBRATION SUPPRESSION AND REDUCTION OF WALK TENDENCY IN HORIZONTAL AXIS WASHING MACHINES USING SEMI-ACTIVE AND ACTIVE SUSPENSION CONTROL METHODS

M.Sc. Thesis by
Dilek BAYRAK, Mech.Eng.

Department : MECHANICAL ENGINEERING
Programme: MACHINE THEORY AND CONTROL

JUNE 2002

İSTANBUL TECHNICAL UNIVERSITY ★ INSTITUTE OF SCIENCE AND TECHNOLOGY

VIBRATION SUPPRESSION AND REDUCTION OF WALK TENDENCY IN HORIZONTAL AXIS WASHING MACHINES USING SEMI-ACTIVE AND ACTIVE SUSPENSION CONTROL METHODS

M.Sc. Thesis by
Dilek BAYRAK, Mech.Eng.

(503991405)

Date of submission : 10 May 2002

Date of defence examination: 5 June 2002

Supervisor (Chairman): Prof. Dr. Levent GÜVENÇ

Members of the Examining Committee Prof. Dr. Yılmaz ÖZTÜRK (İ.T.Ü)

Prof. Dr. Ahmet KUZUCU (İ.T.Ü)

JUNE 2002

İSTANBUL TEKNİK ÜNİVERSİTESİ ★ FEN BİLİMLERİ ENSTİTÜSÜ

YATAY EKSENLİ ÇAMAŞIR MAKİNALARINDA YARI-AKTİF SÜSPANSİYON KONTROL METODU KULLANILARAK TİTREŞİMİN SÖNÜMLENMESİ

YÜKSEK LİSANS TEZİ

Mak. Müh. Dilek BAYRAK
(503991405)

Tezin Enstitüye Verildiği Tarih : 10 Mayıs 2002
Tezin Savunulduğu Tarih : 5 Haziran 2002

Tez Danışmanı : **Prof. Dr. Levent GÜVENÇ**

Diğer Jüri Üyeleri **Prof. Dr. Yılmaz ÖZTÜRK (İTÜ)**

Prof. Dr. Ahmet KUZUCU (İTÜ)

HAZİRAN 2002

ACKNOWLEDGEMENT

I would like to thank my adviser, Prof. Levent Güvenç, for his help and support throughout my study. Also, I am thankful to instructors for their support of this work. In addition, I am grateful to Mr. Kerem Erenay, Research Engineer of Arçelik A.Ş. for their close help in letting me utilize laboratory equipment and computers and in making them available when required. I also wish to extend my sincere thanks to my friends Neslihan Akbaba, M. Erhan Arslan, Edvin Çetegen, Gökhan Balık, Ayşe Zaloğlu, Gülay Özcan, Hakan Ersoy and Yusuf Cunedioğlu for their kind help and backing. Finally, I would like to thank my family for their endless support and patience throughout my studies.

May 2002 Dilek Bayrak

TABLE OF CONTENTS

ABBREVIATIONS

DAQ	:	Data Acquisition System
DC	:	Direct Current
DR	:	Delayed Resonator
ER	:	Electrorheological
KE	:	Kinetic Energy
MR	:	Magnetorheological
PE	:	Potential Energy
PI	:	Proportional Integral
RPM	:	Revolution per Minute
SDOF	:	Single Degree of Freedom

LIST OF TABLES

LIST OF FIGURES

LIST OF SYMBOLS

$\mathbf{b(s)}$	: Repetitive compensator transfer function
$\mathbf{B}$	: Damping present in the rotating system
$\mathbf{c}$	: Damping
$\mathbf{c_{eq}}$	: Equivalent viscous damping
$\mathbf{f}$	: Frequency
$\mathbf{F_c}$	: Control force
$\mathbf{F_C}$	: Coulomb friction force
$\mathbf{F_{frs}}$	: Resistive sliding force
$\mathbf{F_{hor}}$	: Horizontally transmitted force
$\mathbf{F(t)}$	: Centrifugal force
$\mathbf{F_{ver}}$	: Vertically transmitted force
$\mathbf{F_V}$	: Viscous damping force
$\mathbf{g}$	: Gravitational acceleration
$\mathbf{G_p(s)}$	: Compensated plant transfer function
$\mathbf{H(r)}$	: Dynamic factor
$\mathbf{J}$	: Total inertia of the rotating system
$\mathbf{J_{deng}}$	: Inertia of the balanced laundry
$\mathbf{J_{dengsiz}}$	: Inertia of the unbalanced laundry
$\mathbf{J_{dsm}}$	: Inertia of the motor-shaft-drum assembly
$\mathbf{k}$	: Stiffness
$\mathbf{k_{eq}}$	: Equivalent stiffness
$\mathbf{K}$	: Gain
$\mathbf{K_I}$	: Integral gain
$\mathbf{K_p}$	: Proportional gain
$\mathbf{m}$	: Mass
$\mathbf{m_{dengsiz}}$	: Unbalanced mass
$\mathbf{m_u}$	: Unbalance eccentricity
$\mathbf{M}$	: Equivalent mass
$\mathbf{M_s}$	: Multiplying factor
$\mathbf{P(s)}$, $\mathbf{Q(s)}$	: Polynomials of s
$\mathbf{q(s)}$	: Low pass filter
$\mathbf{r}$	: Non-dimensional excitation
$\mathbf{R(\omega)}$	: Regeneration spectrum
$\mathbf{S(s)}$	: Sensitivity function
$\mathbf{S_R(s)}$	: Repetitive control system sensitivity function
$\mathbf{T_D}$	: Time delay
$\mathbf{T_L}$	: Load torque
$\mathbf{V_{max}}$	: Maximum voltage applied to the motor
$\mathbf{x_o}$	: Excitation amplitude
$\mathbf{X}$	: Displacement amplitude
ω	: Rotational speed of the drum
ω_n	: Undamped natural frequency

μ	:	Coefficient of friction
ζ_{eq}	:	Equivalent damping ratio
τ	:	Time constant
υ	:	Voltage applied to the current driver

YATAY EKSENLİ ÇAMAŞIR MAKİNALARINDA YARI-AKTİF SÜSPANSİYON KONTROL METODU KULLANILARAK TİTREŞİMİN SÖNÜMLENMESİ

ÖZET

Çamaşır makinalarında tambur içerisinde çamaşırın düzgün dağılmaması nedeniyle ortaya çıkan dengesiz yük dağılımı merkezkaç bir etki oluşturmaktadır. Dengelenmemiş yük dağılımıyla oluşan merkezkaç etkinin büyüklüğü tamburun hızıyla artan titreşimlere neden olur. Genliği en yüksek olan titreşimler sıkma devrine geçiş sırasında olmaktadır. Bu çalışmada, titreşim genliğini azaltmak için şu ana kadar çamaşır makinasının süspansiyon sisteminde kullanılan kuru sürtünmeli sönümleyici yerine manyetoreolojik MR özellikli sönümleyici kullanılması önerildi. Süspansiyon sisteminin iki serbestlik dereceli modeline literatürden alınan MR sönümleyici modeli monte edilerek yarı-aktif süspansiyon sistemi oluşturuldu. İki serbestlik dereceli yarı-aktif ve pasif süspansiyon modellerinin performansları, titreşim genlikleri ve dikey doğrultuda iletilen kuvvetler göz önüne alınarak incelendi. Bundan sonra açık çevrim yarı-aktif kontrol metodu kullanılarak MR sönümleyicili süspansiyon modelinin davranışı ele alındı. Daha sonra yay, sönümleyici ve kütleden oluşan iki serbestlik dereceli pasif süspansiyon modeline değişik aktif titreşim kontrol teknikleri uygulandı. Son olarak ele alınan her bir kontrol metodunun, dengelenmemiş yük dağılımıyla oluşan titreşimleri gidermedeki etkinliği değerlendirildi.

VIBRATION SUPPRESSION AND REDUCTION OF WALK TENDENCY IN HORIZONTAL AXIS WASHING MACHINES USING SEMI-ACTIVE AND ACTIVE SUSPENSION CONTROL METHODS

SUMMARY

The main source of vibration problems in washing machines is due to the centrifugal forces of the rotating unbalanced laundry. These centrifugal forces generate vibrations whose amplitudes increase with the rotational speed of the drum and reach a peak during the transient period from washing to spin-extraction. The use of magneto-rheological dampers in the drum suspension is considered here in place of the customarily used passive dampers to enhance vibration suppression. In this thesis, a MR damper model taken from the literature is used along with a linear single degree of freedom model of the suspension system of the washing machine. Performances of both passive and semi-active suspension system models of the washing machine regarding displacement amplitude and the vertically transmitted force are investigated first. After that, an open-loop semi-active control method is implemented on the linear single degree of freedom model of the suspension system including MR damper in place of viscous damper. Finally, active vibration control methods are applied to the passive suspension model consisting of a spring, viscous damper and mass and effectiveness of each control method in suppressing the vibrations created by unbalanced laundry is evaluated.

1. INTRODUCTION

The washing machines in the market can be classified as horizontal axis and vertical axis according to the axis of rotation of their drums. The horizontal axis washers are more common in European countries while vertical axis washers are more popular in the USA and far east countries. The walk problem of both horizontal and vertical axis washers was investigated using simple models by Conrad and Soedel (1995). It was shown that the vertical axis washers tend to walk in a bounded region while the horizontal ones tend to walk in an unbounded fashion. Horizontal axis washers are, nevertheles, preferred in several countries as they consume less water, detergent and electrical energy. Being space savers, the horizontal axis washers are also very suitable for installation under kitchen or bathroom counters. To take full advantage of horizontal axis washers, their walk tendency has to be minimized. Conrad and Soedel (1995) consider the simplified horizontal axis washing machine for the constant spin speed and unbalanced laundry over the time. In their work, they assumed a Coulomb dry friction model with a constant coefficient of friction and assumed that the washing machine remains in contact with the floor. In fact, for the 3D model of the washing machine, coefficient of friction present on each foot of the washing machine changes according to the floor properties. Moreover, the reaction forces applied to each foot of the washing machine alter with respect to the position of the unbalanced laundry. As a result, the walking direction of the washing machine changes by the above mentioned factors. However, to simplify the theoretical analysis, the single degree of freedom suspension model of the horizontal axis washing machine is used for investigating the walk tendency of the horizontal axis washer through the washing cycle.

The main source of vibration problems in washing machines are due to the centrifugal forces of the rotating unbalanced laundry. The magnitude of these centrifugal forces depends on the location and the weight of the unbalanced laundry as well as the rotational speed of the drum. All these factors affecting the magnitude of the centrifugal forces vary during the operation of the washing machine. To damp the vibrations generated by the centrifugal forces, friction type shock absorbers are being used. However, these shock absorbers fail to compensate for vibrations whose amplitudes change during the operation of the washing machine. During the resonance condition (the beginning and at the end of the spin cycle) at which vibrations and forces that are transmitted through the suspension unit reach their maximum values, increased damping is needed to attenuate vibrations generated and to reduce the amount of the horizontally transmitted forces which can cause sliding (walk) of the cabinet. On the other hand, optimum damping is required for minimal force transmission after the drum reaches spin speed. To solve the conflicting requirement of high damping during the resonance condition and low damping during the spin cycle the use of variable damping devices like MR dampers can be used. In a magnetorheological (MR) damper, a magnetorheological fluid whose rheology varies with the applied magnetic field is used. Numerous models have been developed for MR dampers and corresponding mechanical models have also been proposed for them.

These thesis concentrates on semi-active and active suspension control methods for vibration suppression and for reducing the walk tendency of horizontal axis washers. In this thesis, the single degree of freedom model of the washing machine suspension system is used in order to simplify the theoretical analysis for passive, semi-active and active suspension systems. First, performances of both an optimum passive suspension system model available in the literature and a semi-active suspension system model consisting of a spring and MR damper are invastigated concentrating on displacement amplitude and the vertically transmitted force. After that, semi-active and active vibration control methods are implemented in a simulation study to the washing machine suspension system and the effectiveness of each method in suppressing the vibrations created by unbalanced laundry is evaluated.

The organization of the thesis is as follows. In Chapter 2, information on both the physical and mathematical models of a washing machine suspension system and the control algorithms developed for semi-active systems is given. Using the single dgree of freedom model of a washing machine suspension system formed by reducing the system to a set of masses, springs and shock absorbers, the effect of the characteristics of the suspension system on the washing machine performance is examined. In Chapter 3, the effects of the unbalance on the vibration of the tub and on the motor of the washing machine are discussed. In Chapter 4, information about both controllable fluids and the devices which make use of their unique properties is given and models developed for these controllable devices are investigated in detail. Comparison of passive and semi-active vibration control is analyzed first in Chapter 5 and then active control algorithms are implemented on the single dgree of freedom model. The thesis ends with the conclusions summarized in Chapter 6.

2. MODELLING PRIMARY SUSPENSION AND VIBRATION CONTROL

This section gives information on both the physical and mathematical models of a washing machine suspension system and control algorithms developed for semi-active systems.

The simplified physical model of a washing machine suspension system has been formed by reducing the system to a set of masses, springs and shock absorbers using simplifying assumptions by Türkay and Taşpınar (1995). The simplified physical model is presented in Figure 2.1. The total mass of the oscillating parts composed of the tub, drum, pulley, motor, heater, counter weights and the laundry is denoted by M. The mass of the unbalanced load which determines the magnitude of the centrifugal force is denoted by m_u. The external forces on the oscillating mass are transmitted by the suspension springs, shock absorbers and front door bellows. The total force can be decomposed into spring and viscous damper element forces. The motor generates a torque that usually rotates the drum with a pulley and belt arrangement. Note that the motor drives the drum directly in a direct drive arrangement which is also considered in this thesis. The torque produced at the drum shaft rotates the drum.

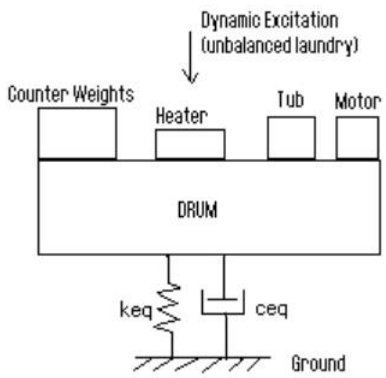

Figure 2.1. Simplified physical model of the system

The tub of the washing machine system has six degrees of freedom of rigid body motion. To simplify the theoretical analysis for implementation of vibration control algorithms, a single degree of freedom (SDOF) suspension model that parallels that proposed by Türkay and Taşpınar (1995) is used throughout this thesis, and explained in detail in subsequent sections.

2.1. Physical Model

The horizontal axis front loading washing machine system considered in this study is schematically represented as in Figure 2.2

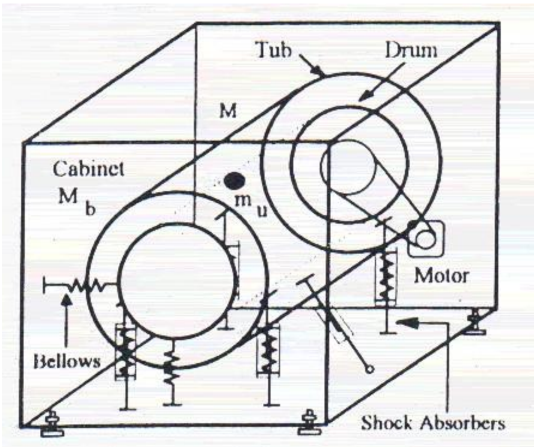

Figure 2.2 Schematic view of the washing machine (from Türkay and Taşpınar, 1995)

In general, the washing machine system can be investigated in three main groups. These are the washing unit, suspension unit and the body or cabinet. The washing unit consists of a horizontal tub, an electric motor located at the bottom, concrete counter weights located at the front and top, a horizontal drum which rotates on its axis and in alternating directions, a shaft which is connected to the tub by bearings and rigidly connected to the drum, a belt-pulley mechanism located at the back and a heater located between the tub and the drum. The suspension unit supporting the drum-tub-motor assembly is composed of two dry friction shock-absorbers, four springs and circular plastic bellows. The cabinet consists of a control panel, a detergent dispenser which resembles a drawer located at the front of the washing machine, a pump, a drain hose and circular door through which laundry is placed. The cabinet standing with four plastic supports (or feet) on the ground encloses the suspension, washing unit and the other electrical and mechanical elements of the washing machine.

2.1.1 Shock absorbers

The dry friction shock absorbers are connected to the tub and the cabinet by revolute joints. They are used to dissipate energy to modify the response of the system to shocks and excitation forces. They are considered to operate with a combined viscous and Coulomb friction principle. The resistive force generated by these absorbers was expressed in (Türkay, 1993) as;

$$F_A = -(F_V + F_C) \tag{2.1}$$

where F_V is the viscous damping force and F_C is the coulomb friction force.

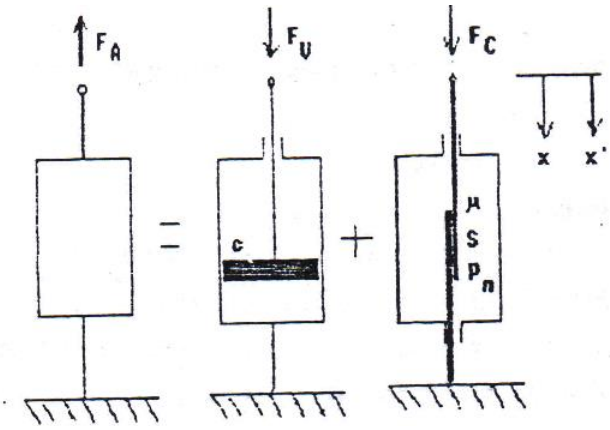

Figure 2.3. Shock absorber model (from Türkay, 1993)

Viscous damping provided by these devices is due to the dissipation of energy that occurs as the system is resisted by a force that has a magnitude proportional to the magnitude of the velocity and a direction opposite to its direction. This effect occurs when the piston of the damper decreases the volume and increases the pressure of the fluid in the damper. The fluid tries to pass from a narrow space and exerts a resistive force. The Coulomb friction force results from the relative motion of two solids members held together under pressure and opposes the intended direction of motion.

2.1.2 Bellows

The bellows is a circular component that connects the washing machine tub to the outer body at the front door of the machine and maintains the water in the tub. It acts as a non linear spring and damping element.

2.2 Simplified Mathematical Model of the Washing Machine Suspension System

The actual model of the washing machine shown in the Figure 2.2 is simplified for vibration control in the light of assumptions that are backed by experimental results (Türkay and Taşpınar, 1995). A single degree of freedom model (SDOF) consisting of a mass, a spring, and an equivalent viscous damper is formed for simplicity of initial analysis rather than using a model having six degrees of freedom (Türkay, 1995).

The simplified model of the washing machine replacing the dry friction shock absorbers with an equivalent viscous damping is shown in Figure 2.4

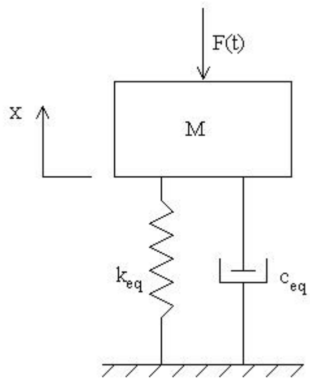

Figure 2.4. Simplified SDOF Linear Model

The equation of motion of the single degree of freedom model is given as

$$M\ddot{x} + c_{eq}\dot{x} + k_{eq}x = F(t) \qquad (2.2)$$

where M, c_{eq} and k_{eq} denote equivalent mass, damping and stiffness parameters of the simplified system, respectively. In this equation, $F(t)$ represents the centrifugal force generated by the unbalanced laundry and is given by

$$F(t) = F_o \sin\omega t = m_u\omega^2 Sin\omega t \qquad (2.3)$$

Where m_u and ω are the unbalanced eccentricity (unbalanced mass times eccentricity) and the drum spin speed, respectively.

Model parameters of the simplified single degree of freedom system are taken from the work of Türkay and Taşpınar (1995) and are listed in Table 2.1

Table 2.1. Parameters for the simplified model (from Türkay and Taşpınar, 1995)

PARAMETER	VALUE
Tub-drum mass, M	61 kg
Eccentric mass, m_u	0.7 kg m
Stiffnes, k_{eq}	16000 N/m
Equivalent damping, c_{eq}	515 Ns/m
Undamped natural frequency, ω_n	16 rad/sec
Non-dimensional spin-dry speed, $r = \omega / \omega_n$	54/16 = 3.4
Equivalent damping factor, $\zeta_{eq} = c_{eq} / 2\sqrt{k_{eq} M}$	0.26

2.3 Passive Suspension and Passive Vibration Suppression

Until now, vibration control of washing machines has been implemented in a passive manner by adjusting the mass, stiffness and damping parameters of the suspension unit. To suppress the amplitude of excitations created by unbalanced laundry, a large amount of mass in the form of concrete or cast iron are added to the system to increase the total mass of the tub-drum assembly. The main problem encountered in the washing machine is walking of the washing machine caused by horizontally transmitted forces. From equation (2.2) the steady state (static) response of the system to forces generated by unbalanced laundry can be obtained assuming a solution:

$$x(t) = x(\omega)e^{i\omega t} \tag{2.4}$$

and substituting (2.4) into equation (2.2). After some algebraic manipulations and letting *F(t)* equal $F_o e^{i\omega t}$ we get the steady state amplitude as;

$$x(\omega) = \frac{F_0}{k_{eq}}\left|H(j\omega)\right| = \frac{F_0 / k_{eq}}{\sqrt{(1-r^2)^2 + (2\zeta_{eq} r)^2}} \tag{2.5}$$

$$x(t) = x(\omega).sin(\omega.t - \varphi) \tag{2.6}$$

where

$$\varphi = tan^{-1} \frac{2\zeta r}{1 - r^2} \tag{2.7}$$

After obtaining the steady state amplitude of the system, we can compute the force transmitted to the base of the washing machine. From figure 2.4, it is deduced that the vertically transmitted force can be acquired as:

$$F_{ver}(t) = c_{eq}\dot{x}(t) + k_{eq}x(t) \tag{2.8}$$

Putting the value of x(t) from equations (2.5)-(2.7) into equation (2.8), the steady state amplitude of the vertically transmitted force is found to be

$$F_{ver}(\omega) = m_u.\omega^2 \frac{\sqrt{1 + (2\zeta r)^2}}{\sqrt{(1 - r^2)^2 + (2\zeta r)^2}} \tag{2.9}$$

Figure 2.5 illustrates a typical wash cycle for a horizontal axis washing machine in terms of drum rotational speed in revolutions per minute (RPM) versus time. The cycle from T1 to T2 represents a wash cycle in which the rotating member (drum assembly) executes reciprocating rotations. As the drum rotation accelerates into the spin cycle, represented by the period from T3 to T4, the drum assembly passes through a resonance condition (critical speed), which is shown in Figure 2.6 between speed points A and B that results in the largest transmitted force. The washing machine operation may include more wash and spin-extraction cycles depending on its model and the washing program that is chosen. The critical speed may, thus, be reached more than once during a washing operation.

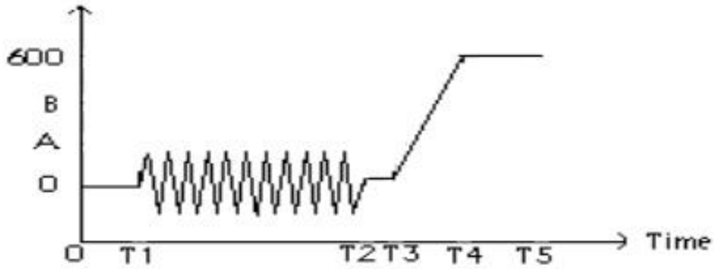

Figure 2.5. A typical wash cycle for a horizontal axis washing machine

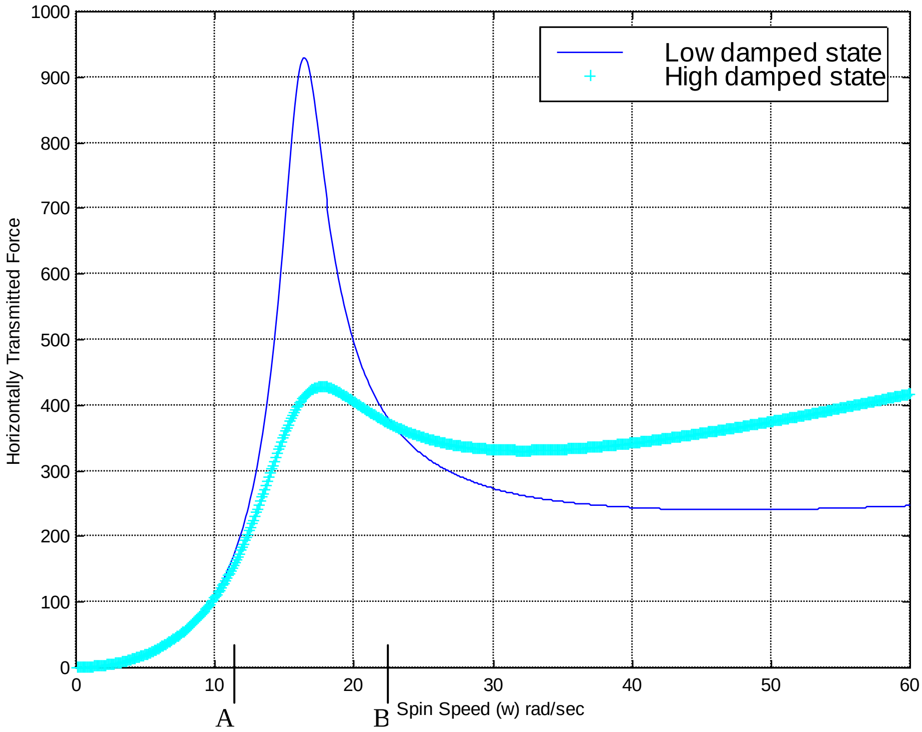

Figure 2.6 Horizontally transmitted force versus spin speed

The sliding of the cabinet is likely to happen during the resonance condition of the wash cycle, since during this condition, the horizontal forces transmitted to the cabinet through the suspension of the washing machine can exceed the frictional force in the same direction. The horizontally transmitted force is assumed to be approximately one quarter of the vertically transmitted one. Using equation (2.9), the horizontally transmitted forces for two damping values are obtained and plotted as in Figure 2.6. It can be seen that increased damping is advantageous during the resonance condition (the beginning and at the end of the spin cycle) which is shown in Figure 2.6 between speed points *10 rad/s* and *25 rad/s*. However, increased damping will cause the cabinet to slide after the drum reaches spin speed, so low damping is required for minimal force transmission after the drum reaches spin speed. As a result, the passive suspension system provides design simplicity and cost effectiveness, but the performance limitations mentioned above are also inevitable.

2.4 Vibration Suppression Mechanisms

To reduce undesirable vibrations in mechanical systems generated by external disturbances, numerous vibration suppression mechanisms are developed and implemented. In this study, we mention passive, semi-active and active suspension systems and vibration absorbers.

2.4.1 Vibration absorbers

Among the possible ways of reducing undesirable vibrations in mechanical systems, vibration absorbers are used when internal modification to the main system are difficult to carry out.

The passive vibration absorber is itself a passive vibrating system, which consists of a mass, a spring and perhaps a damper. The model of a passive vibration absorber is shown in Figure 2.7

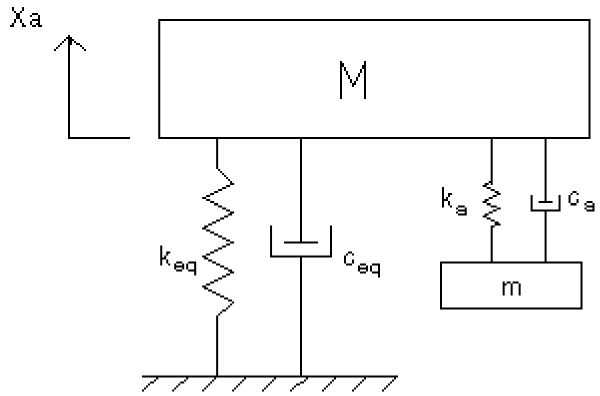

Figure 2.7. Passive Vibration Absorber

Passive vibration absorbers attached to primary structures have long been used to suppress vibrations generated by external disturbances. They are quite effective within a narrow band of frequencies that are tuned for (Elmali, Renzulli and Olgaç, 2000). For the vibration created by excitations (i.e., of single harmonic), the ground rule of absorption is that the primary structure can be brought to rest if the vibration absorber attached to it has ideal resonance properties at the frequency of excitation (Elmali, Renzulli and Olgaç, 2000). The ideal resonance can be achieved only if the absorber has no damping, which is often not feasible because every physical system has some degree of damping. As a result, passive vibration absorbers can not completely suppress the tonal vibrations (Elmali, Renzulli and Olgaç, 2000). Furthermore, passive vibration absorbers are not effective if a wide frequency range of excitation is present since combined system (primary system + passive vibration absorber) exhibits large resonance response at other frequencies (Soom and Lee, 1983)

Recently, there is a growing interest in active vibration absorbers. However, a common design methodology for general usage of active vibration absorbers has not been established yet (Elmali, Renzulli and Olgaç, 2000). Elmali, Renzulli and Olgaç (2000) developed an active vibration absorption technique called the *Delayed Resonator* (DR) that uses a time delayed position feedback as control logic. When the proportional gain and the feedback delay are properly selected, this simple control adjusts the absorber to become a resonator at a desired frequency that is tunable in real time (Elmali, Renzulli and Olgaç, 2000). When attached to a primary structure, the resonator removes all oscillations at the resonance frequency at the point of attachment. A single degree of freedom system with a delayed resonator is shown in Figure 2.8.

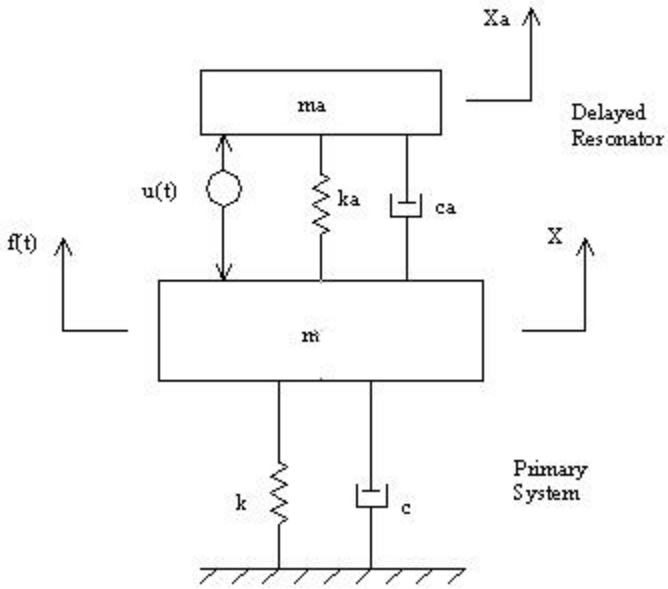

Figure 2.8. SDOF Primary System with PR Resonator (from Olgaç, 2000)

2.4.2 Semi-active suspension and semi-active vibration control

Semi-active suspension systems combine the best features of both active and passive control systems and thus offer the reliability of passive systems by maintaining the versatility and adaptability of fully active systems.

Washing machines employing new controllable dampers of the electrorheological and magnetorheological type have been developed recently. These dampers are classified as semi-active dampers since they can only provide dissipative forces proportional to the voltage applied to them. These controllable devices have a relatively simple mechanism and small response time. The further development of these devices has therefore been progressing rapidly. Moreover, the main characteristic of these devices is that they vary their dynamic properties with a minimal amount of power (Spencer and Sain, 1997). Also, they are expected to offer effective performance over a variety of amplitude and frequency ranges. The other attractive features are their simple mechanism, reliability and stability (Dyke, Launa and Jansen, 1997).

In this study, a semi active suspension system consisting of the conventional spring element and a controllable damper, MR damper is used. Semi active suspension system of the simplified washing machine model is illustrated in Figure 2.9.

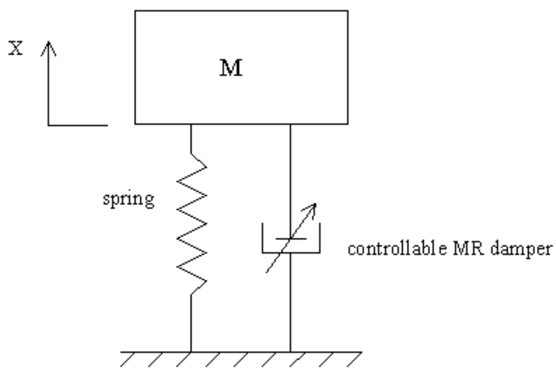

Figure 2.9. The Semi-active Suspension

In this type of semi-active suspension system, the fluid's magnetorheological property allows the effective viscosity of the working fluid inside the damper to be altered by varying the applied magnetic field. The level of damping present in the system can be determined and adjusted by an electronic controller during the operation of the washing machine.

Since a decade, there have been modern vibration control techniques that have found commercial applications. These developments have been due to the possibility of electronically controlling the characteristics of new actuators such as electromagnetic, piezoelectric, semi-active hydraulic and ER or MR fluid based devices. Among these, piezoelectric actuators are not applicable to systems having large vibration amplitude such as the case of a washing machine. The hydraulic shock absorbers using electromagnetic actuator to vary valve opening need a hydraulic system to be operated. The hydraulic system consisting mainly of pressure control valves, accumulator, oil reservoir, check valves, etc adds additional cost to the washing machine system, so the semi-active hydraulic shock absorbers are not applicable for washing machines. On the other hand, MR devices can generate forces up to *3000 N* with a peak power of less than *10 Watts* and are simpler to design and manufacture and less costly than their counterparts. Therefore, in this study, the MR devices are incorporated into the washing machine suspension system in order to provide the required damping values for the whole spectrum of speeds used.

Semi-active vibration control method relies on changing the characteristic of the actuator using a low control energy input. This control can be implemented in an open-loop or closed-loop manner depending on the dynamics and excitation of the system to be controlled.

Numerous control algorithms have been adopted for semi-active systems. The one concerning the washing machine system is Taşpınar's (1992) work that presents a open-loop semi-active vibration control method of a simplified single degree of freedom model of a horizontal-axis washing machine. In this work, the semi active control technique is formulated off-line to optimize the damping and stiffness variables in order to minimize the vibration amplitude of a simplified washing machine model subject to resistive sliding force constraint of the cabinet. Then, these optimum values are stored and applied on-line to the tub employing an open-loop strategy.

2.5. Semi-Active Vibration Control of the Washing Machine Suspension System

In this optimization problem, avoiding the sliding of the cabinet with respect to ground was taken as a constraint. Sliding would occur if the resultant of horizontal forces transmitted to the ground is greater than the resultant of the frictional force in the same direction. The resistive sliding force vector is defined in Taşpınar (1993) as;

$$F_{rsf} = \mu.\sum F_{ver} - \sum F_{hor} \tag{2.10}$$

$$\mu \sum F_{ver} \geq \sum F_{hor}$$

$$F_{rsf} \geq 0$$

where μ, $\sum F_{ver}$, and $\sum F_{hor}$ are the friction coefficient between the base of the machine and the floor and the resultant of vertically and horizontally transmitted dynamic force vectors, respectively.

In order to determine the coefficient of friction, an experimental study was made at a manufacturer of a washing machine company. The machine was pulled horizontally with an increasing force applied parallel to the floor The total mass of the washing machine used was about *77 kg*. On a dry characteristic bathroom floor, the machine started to move in the horizontal direction when the applied force was about *355 N* On the other hand, the motion was activated with *225 N* when the floor was wet. Thus, the wet and dry floor coefficient of friction were calculated as

$$\mu = \frac{\left(\sum F_{hor}\right)_{impending\_motion}}{\left(\sum F_{ver}\right)_{impending\_motion}} = \frac{225}{77 * 9.81} = 0.298 =\sim 0.3 \tag{2.11}$$

$$\mu = \frac{\left(\sum F_{hor}\right)_{impending\_motion}}{\left(\sum F_{ver}\right)_{impending\_motion}} = \frac{355}{77 * 9.81} = 0.47 =\sim 0.5 \tag{2.12}$$

The coefficient of friction will be taken as *0.4* here in order to obtain more realistic results.

The cabinet of the washing machine will not move if the resistive sliding force is positive, $F_{rsf} \geq 0$. By using equation (2.10) we can compute the resistive sliding force for the actual washing machine. For the simplified model, we have already calculated the static value of the vertically transmitted force as in equation (2.9). Based on the experimental observations in a manufacturer of washing machines, the horizontally transmitted force was seen to be approximately one quarter of the vertically transmitted one. Thus, the resistive sliding force of the single degree of freedom model can be obtained as

$$F_{rsf}(\omega) = \mu W - 0.25 F_{ver}(\omega) \tag{2.13}$$

$$F_{rsf}(\omega) = \mu W - 0.25 m_u \frac{\omega^2 \sqrt{1+(2\zeta r)^2}}{\sqrt{\left(1-r^2\right)^2 + \left(2\zeta r\right)^2}} \tag{2.14}$$

where W denotes the total weight of the washing machine system and is used instead of $\sum F_{ver}$ in (2.10) assuming static conditions.

The static displacement amplitude and resistive sliding force F_{rsf} of the model that are computed for different damping and stiffness values using equations (2.5) and (2.14) are displayed in Figures 2.10 to 2.13. In Figure 2.10 and 2.11, it is seen that holding the damping at its nominal value and increasing the stiffness increases the displacement amplitude and causes sliding of the cabinet for k = 32000 N/m. Hence, a soft spring gives a better performance than a hard spring regarding the amplitude of vibration and walking of the cabinet. However, this may not be permissible in a given design since a threshold value of minimum stiffness is necessary to provide the static load carrying capacity of the suspension system. On the other hand, holding the stiffness at its nominal value and increasing the damping decreases the static displacement amplitude. However, the damping values of c = 750 Ns/m and c = 1000 Ns/m, at around $\omega = 400$ rpm (42 rad/sec) and $\omega = 500$ rpm (52 rad/sec), respectively cause the cabinet to slide. Consequently, from Figure 2.12 and 2.13, it is understood that while increased damping is advantageous during resonance, increased damping will cause more force to be transmitted after the drum reaches spin speed. Therefore, low damping is required for minimal force transmission after the drum reaches spin speed.

To find the appropriate damping and stiffness values for minimum force transmission throughout the washing machine cycle, Türkay and Taşpınar (1995) formulated an optimization problem by taking the displacement amplitude as their objective function and the resistive sliding force as a constraint. Considering the robustness of the cabinet and the possible changes which may occur in the mechanical parameters due to wear, thermal effects, change in friction coefficient a safety margin of 50 N ($F_{rsf} \geq 50N$) was included in their constraint equation.

Türkay and Taşpınar (1995) optimized the damping value as a function of the spin speed by holding the stiffness and all other parameters constant at their nominal values. The optimum damping values with respect to rotational speed of drum found by Türkay and Taşpınar (1995) and corresponding graphs for the optimum damping case are displayed in Figure 2.14. It is seen from Figure 2.10 and Figure 2.14 that the resonant peak of 0.023 *m* of passive suspension system having the damping of 515 Ns/m and stiffness of 16000 N/m (see Figure 2.10) is damped sufficiently if maximum damping is applied until *250 rpm* (see Figure 2.14). After the drum speed of *250 rpm*, decreasing the damping reduces the amount of horizontally transmitted forces to the cabinet.

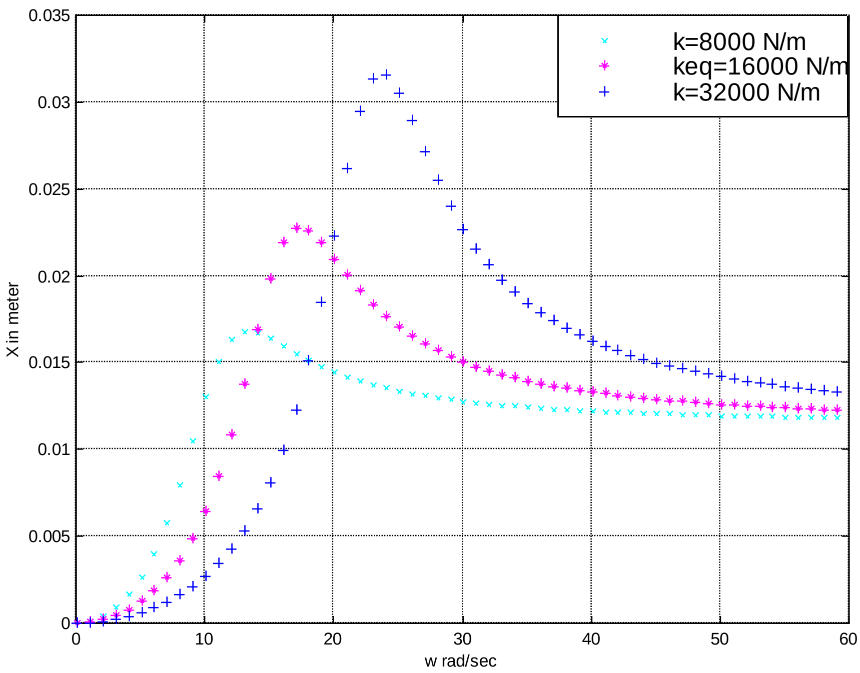

Figure 2.10. Static displacement amplitude vs drum rotational speed

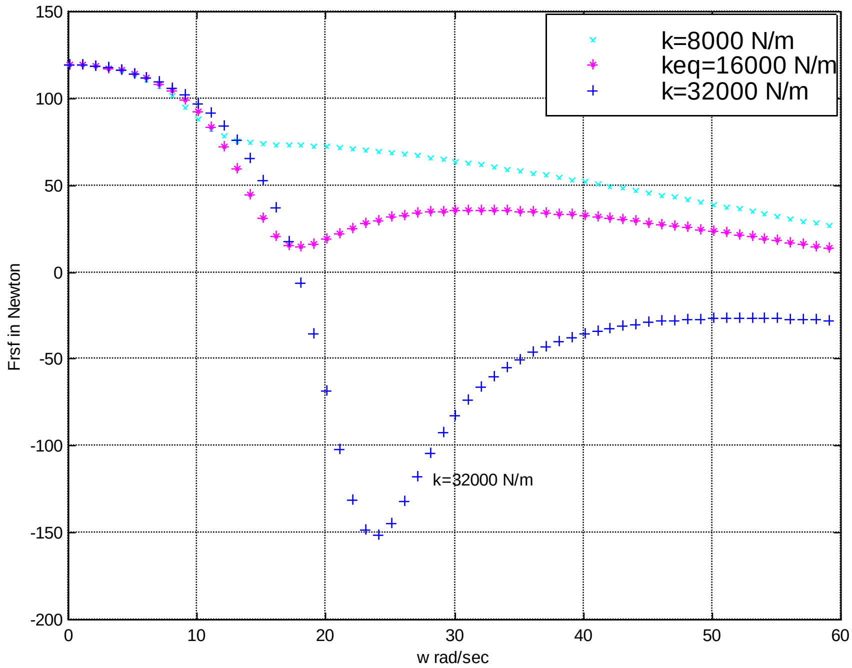

Figure 2.11. Resistive sliding force vs drum rotational speed

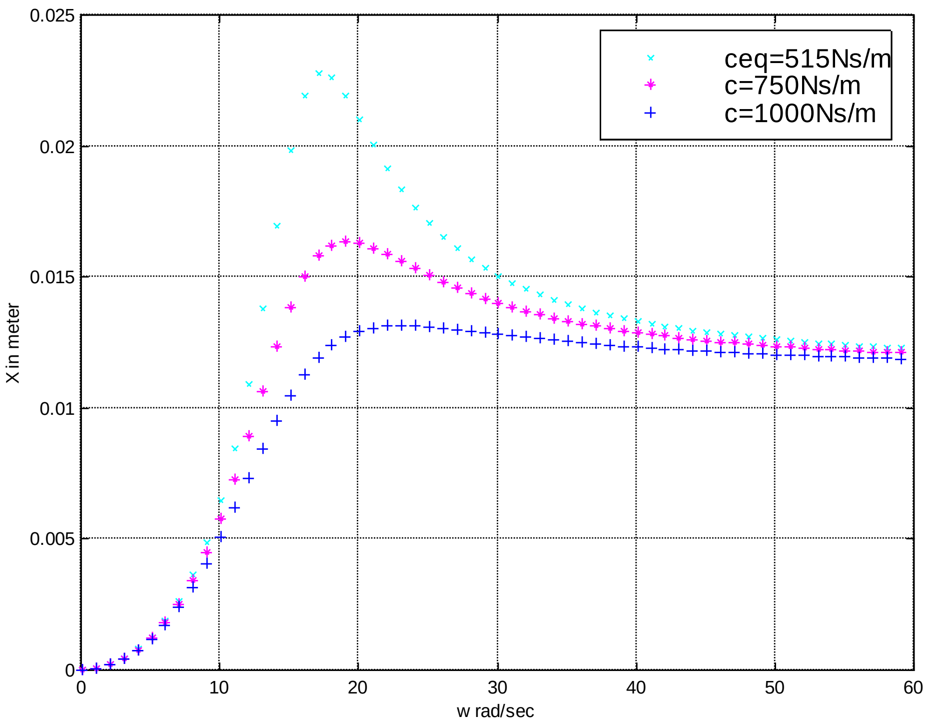

Figure 2.12. Static displacement amplitude vs drum rotational speed

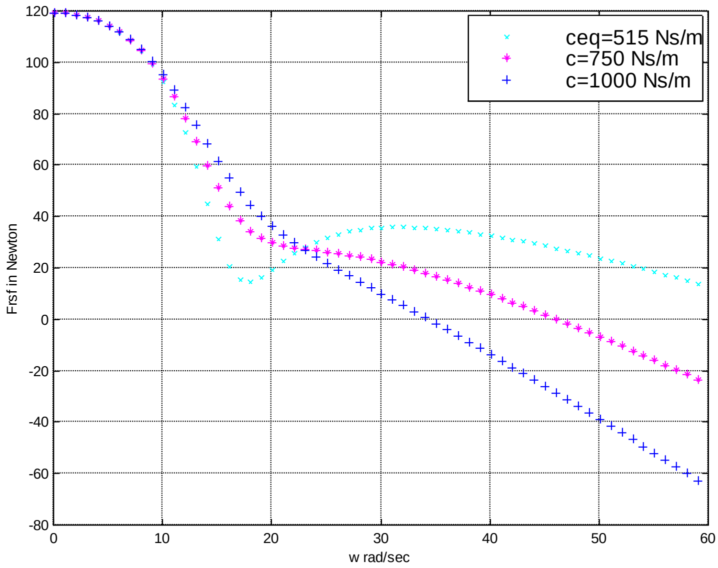

Figure 2.13. Resistive sliding force vs drum rotational speed

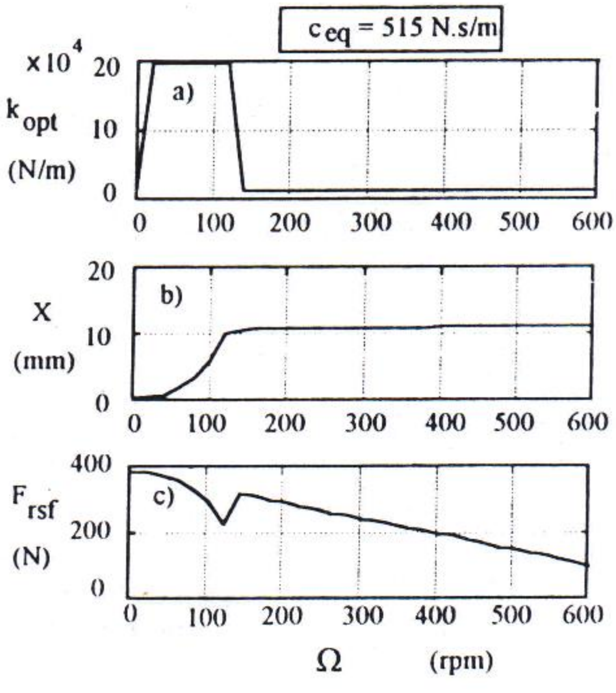

Figure 2.14. Optimum damping, displacement amplitude and F_{rsf} values vs drum rotational speed (from Taşpınar, 1993)

2.6. Skyhook Control Policy

In one of the first examinations of semi-active control, Karnopp (1974) proposed the 'skyhook' damper control algorithm for a vehicle suspension system. The skyhook method offers improved performance over a passive system when applied to a SDOF system.

The skyhook control adjusts the damping level to imitate the effect of a damper connected from the vehicle to a stationary ground, as shown in Figure 2.15.

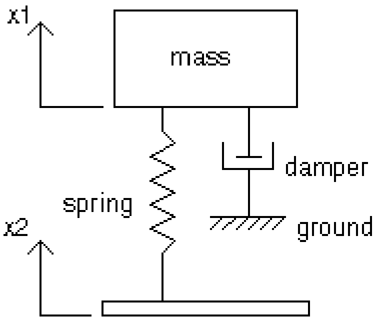

Figure 2.15. Quarter car model with Skyhook Damper

Mathematically, the skyhook control is described as,

$$\dot{x}_1\left(\dot{x}_1 - \dot{x}_2\right) \geq 0 \qquad\qquad c = \text{high damping}$$

$$\dot{x}_1\left(\dot{x}_1 - \dot{x}_2\right) < 0 \qquad\qquad c = \text{low damping}$$

In this equation $\dot{x}_1$ is the velocity of the upper mass. And $\dot{x}_2$ is the velocity of lower mass. This type of skyhook control is called on-off, or bang-bang control since the damper switches back and forth between two possible damping states. When the upper mass is moving up and the two masses are getting closer, the damping constant should ideally be zero. Due to the physical limitations of a practical damper, a low damping constant is used instead. When the upper mass is moving down and the two masses are getting closer, the skyhook control ideally calls for an infinite damping constant. An infinite damping constant is not physically attainable, so in practice, the adjustable damping constant is set to a maximum. The objective of the skyhook control scheme is to minimize the absolute velocity of the upper mass. This is shown in Figure 2.16.

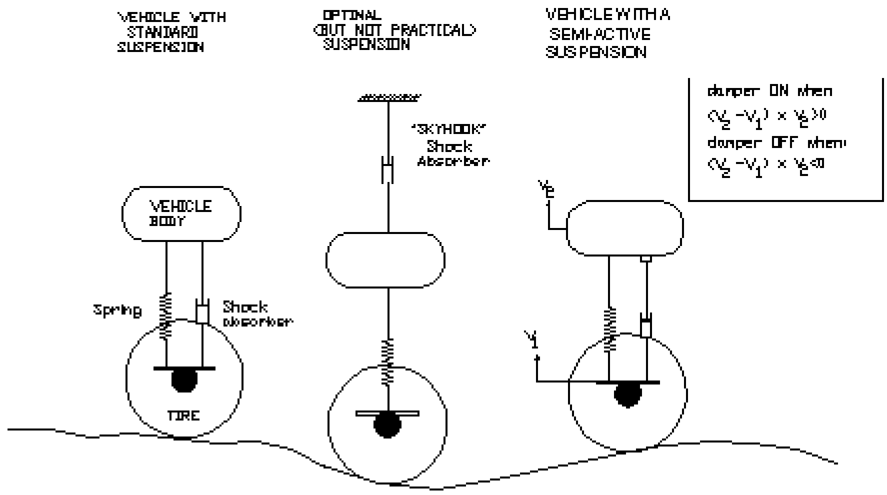

Figure 2.16. Skyhook Control Scheme

More recently, a control strategy based on Lyapunov stability theory has been proposed for electrorheological dampers (Brogan, 1991, Leitmann, 1994). The goal of this algorithm is to reduce the response by minimizing the rate of change of a Lyapunov function. McClamroch and Gavin (1995) used a similar approach to develop a decentralized bang-bang controller. This control algorithm acts to minimize the total energy in the structure. In addition to that, clipped-optimal controllers have been proposed and implemented for semi-active systems by Spencer et. al. (1996).

The above mentioned control algorithms were employed to control a seismically excited structure with n MR dampers. Assuming that the forces provided by the control devices are adequate to keep the response of the primary structure from exiting the linear region, the equation of motion was obtained as:

$$\mathbf{M_s}\ddot{\mathbf{x}} + \mathbf{C_s}\dot{\mathbf{x}} + \mathbf{K_s}\mathbf{x} = \mathbf{U}\mathbf{f} - \mathbf{M_s}\mathbf{G}\ddot{\mathbf{x}}_{\mathbf{g}} \qquad (2.14)$$

where

$\boldsymbol{x}$: vector of the relative displacements of the floors of the structure.

$\ddot{x}_g$: 1D ground acceleration

$\mathbf{f} = [f_1, f_2, \ldots\ldots, f_n]^T$: dampers vector of measured control forces generated by the n MR

$\mathbf{G}$ column vector of ones

$\mathbf{U}$: vector determined by the placement of the MR dampers in the structure

Equation (2.14) can be written in state space form as

$$\dot{\mathbf{z}} = \mathbf{Az} + \mathbf{Bf} + \mathbf{E}\ddot{\mathbf{x}}_{\mathbf{g}} \qquad (2.15)$$

$$\mathbf{y} = \mathbf{Cz} + \mathbf{Df} + \mathbf{v} \qquad (2.16)$$

where

$\boldsymbol{z}$ **:** state vector

$\boldsymbol{y}$: vector of measured outputs

$\boldsymbol{v}$: measurement noise vector

2.7. Control Based on Lyapunov Stability Theory

Leitmann (1994) applied Lyapunov's direct approach for the design of a semi-active controller. The approach requires the use of a Lyapunov function, denoted $V(\mathbf{z})$, which must be a positive definite function of the states of the system $\mathbf{z}$. The origin is assumed to be a stable equilibrium point. According to Lyapunov stability theory, if the rate of change of the Lyapunov function $\dot{V}(\mathbf{z})$ is negative semi-definite, the origin is stable in the sense of Lyapunov. Thus, in developing the control law, the goal is to choose control inputs for each device that will result in making $\dot{V}$ as negative as possible. An infinite number of Lyapunov functions may be selected, that may result in a variety of control laws.

In this approach, a Lyapunov function is chosen of the form:

$$V(z) = \frac{1}{2}\|\mathbf{z}\|^2{}_p \qquad (2.17)$$

$$\|\mathbf{z}\|_p = \left[\mathbf{z}^T\mathbf{Pz}\right]^{1/2}$$

where

$\|\mathbf{z}\|_p$: P-norm of the states defined by

$\boldsymbol{P}$: real, symmetric, positive definite matrix.

In the case of a linear system, to ensure $\dot{V}$ is negative definite, the matrix $\boldsymbol{P}$ is found using the Lyapunov equation:

$$\mathbf{A}^T\mathbf{P} + \mathbf{PA} = \mathbf{Q}_p \tag{2.18}$$

for a positive definite matrix $\mathbf{Q}_p$. The derivative of the Lyapunov function for a solution of (2.15) is

$$\dot{V} = -\frac{1}{2}\mathbf{z}^T\mathbf{Q}_p\mathbf{z} + \mathbf{z}^T\mathbf{PBf} + \mathbf{z}^T\mathbf{PE}\ddot{x}_g \tag{2.19}$$

The only term that can be directly affected by a change in the control voltage is the middle term that contains the force vector, $\boldsymbol{f}$. Thus, the control law which will minimize $\dot{V}$ is

$$\upsilon_i = V_{max}H((-\mathbf{z})^T\mathbf{PB}_i f_i) \tag{2.20}$$

where

$H(.)$: Heaviside step function

f_i : measured force produced by the i th MR damper

$\mathbf{B}_i$: i th column of the $\mathbf{B}$ matrix in (2.15)

This algorithm is classified as a bang-bang controller and is dependent on the sign of the measured control force and the states of the system. To implement this algorithm, a Kalman filter is used to estimate the states based on the available measurements. (i.e., device displacements, device forces, and structural accelerations). Thus, in this algorithm, better performance is expected when measurements of the responses of the full structure are used. However, one challenge in the use of the Lyapunov algorithm is in the selection of an appropriate $\mathbf{Q}_p$ matrix.

2.8 Decentralized Bang-Bang Control

McClamroch and Gavin (1995) used a similar approach to develop the decentralized bang-bang control law for use with an electrorheological damper. In this approach, the Lyapunov function was chosen to represent the total vibratory energy in the structure (kinetic plus potential energy), as in

$$V = \frac{1}{2}\mathbf{x}^T\mathbf{K}_s\mathbf{x} + \frac{1}{2}(\dot{\mathbf{x}} + \mathbf{G}\dot{x}_g)^T\mathbf{M}_s(\dot{\mathbf{x}} + \mathbf{G}\dot{x}_g) \tag{2.21}$$

Using equation (2.14), the rate of change of the Lyapunov function is then

$$\dot{V} = \frac{1}{2}\mathbf{x}^T\mathbf{K}_s\dot{\mathbf{x}} + (\dot{\mathbf{x}} + \mathbf{G}\dot{x}_g)^T(-\mathbf{C}_s\dot{x} - \mathbf{K}_s x + \mathbf{U}\mathbf{f}) \tag{2.22}$$

In this expression, the only way to directly effect $\dot{V}$ is through the last term containing the force vector $\mathbf{f}$. To control this term and make $\dot{V}$ as large and negative as possible (maximizing the rate at which energy is dissipated), the following control law is chosen:

$$\upsilon_i = V_{max}H(-(\dot{\mathbf{x}} + \mathbf{G}\dot{x}_g)^T\mathbf{U}_i f_i) \tag{2.23}$$

where

$\mathbf{U}_i$: i th column of the $\mathbf{U}$ matrix

Since the only non-zero terms in the $\mathbf{U}$ matrix are those corresponding to the location of the MR dampers, this control law requires only measurements of the floor velocities and applied forces. Interestingly, when any of the semi-active devices are located between the ground and first floor, the absolute velocity of the first floor is required. When the control device is located in the upper floors, the interstory velocity is needed. Therefore, to implement this control algorithm, one would approximate the absolute velocity (obtain the pseudovelocity) by integrating the absolute acceleration (Spencer et al., 1997b) using

$$H(s) = \frac{39.5s}{39.5s^2 + 8.89s + 1} \tag{2.24}$$

2.9 Clipped-Optimal Control

The other algorithm that has been shown to be effective for use with the MR damper is a clipped-optimal control approach, proposed by Dyke et al. (1996 c, d, e). The clipped optimal control approach is to design a linear optimal controller $\mathbf{K}_c(s)$ that calculates a vector of desired control forces $\mathbf{f}_c = [f_{c1}, f_{c2}, \ldots\ldots, f_{cn}]^T$ based on the measured structural responses **y** and the measured control force vector **f** applied to the structure; that is :

$$f_c = L^{-1}\{-K_c(s)L\{\begin{matrix} y \\ f \end{matrix}\}\} \tag{2.25}$$

where L{.} represents Laplace transform.

Because the force generated in the MR damper is dependent on the local responses of the structural system, the desired optimal control force f_{ci} cannot always be produced by the MR damper. Only the control voltage υ_i can be directly controlled to increase or decrease the force produced by the device. Thus, a force feedback loop is incorporated to induce the MR damper to penetrate approximately the desired optimal control force f_{ci}.

To induce the MR damper to generate approximately the corresponding desired optimal control force f_{ci}, the command signal υ_i is selected as follows. When the i th MR damper provides the desired optimal force (i.e. $f_i = f_{ci}$), the voltage applied to the damper should remain at the present level. If the magnitude of the force produced by the damper is smaller than the magnitude of the desired optimal force and the two forces have the same sign, the voltage applied to the current driver is increased to the maximum level to increase the force produced by the damper to match the desired control force. Otherwise, the commanded voltage is set to zero. The algorithm for selecting the command signal for the i th MR damper is graphically represented in Figure 2.17 and can be stated as

$$\upsilon_i = V_{max}H(\{f_{ci} - f_i\}f_i) \tag{2.26}$$

Although a variety of approaches may be used to design the optimal controller, H_2 and Linear Quadratic Gaussian methods are advocated because of their successful application in previous studies. The approach to optimal control design is discussed in detail in Dyke (1996).

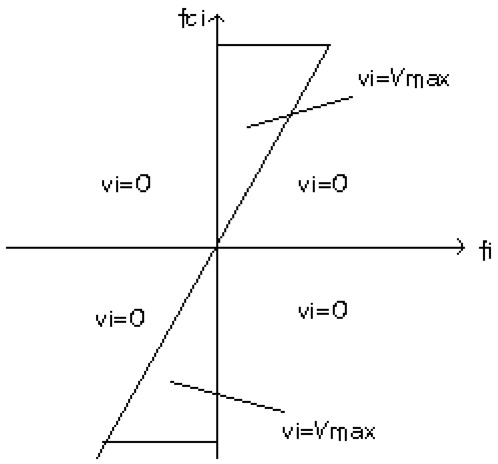

Figure 2.17. Graphical Representation of Algorithm for selecting command signal

2.10 Active Suspension and Vibration Control

In an active suspension, the passive damper or both the passive damper and spring are replaced with a force actuator as illustrated in Figure 2.18.

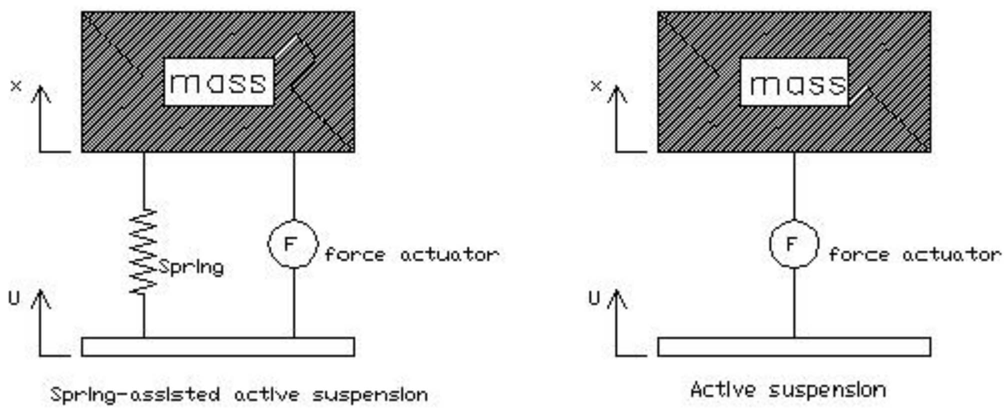

Figure. 2.18. Active suspension

The force actuator is able to both add and dissipate energy from the system, unlike a passive damper, which can only dissipate energy. With an active suspension, the force actuator (e.g., a hydraulic piston, a piezoelectric device, an electric motor) can apply force independent of the relative displacement or velocity across the suspension.

Active vibration control relies on providing large reactive forces through the actuator using closed-loop control. There are various active control methods proposed in the literature each having their own merits. Active vibration control achieves high-level of control with versatility and better performance in the design of vibration suppression systems.

The active and semi-active systems have better vibration suppression performance than the passive ones that are not adaptable to the disturbances. The semi-active system is advantageous over the active one in that it occupies less space, consumes less energy and guarantees stability. Practically, by using the proper real time control algorithm, the semi-active suspension system can achieve performance levels close to the active one. Moreover, semi-active systems not only have a less dangerous failure mode, but are also less complex, less prone to mechanical failure and have much lower power requirements as compared to active systems.

3. THE ORIGIN OF UNBALANCE AND THE NECESSITY FOR ESTIMATION OF THE UNBALANCED MASS IN WASHING MACHINE SYSTEMS

Looseness in roller bearings, shaft eccentricity, bending in shafts and non-homogeneous parts are the main factors causing unbalance in rotating machines. In addition to these, in washing machines, during the spin cycle there is a tendency for the laundry to bunch up and gather on one side of the drum, thus causing unbalance in the rotating system. This unbalance created in the rotating system generates centrifugal forces, the magnitudes of which are directly proportional to the amount of unbalanced laundry, the square of the drum spin speed, and the distance between the rotational axis of the drum and the unbalanced laundry.

The centrifugal forces created by the unbalanced laundry are transmitted to the supporting unit and the basement. If the horizontally transmitted forces due to the centrifugal forces are greater than the floor frictional forces, then sliding of the cabinet occurs this phenomenon is observed especially at high spin speeds. The centrifugal forces that occur while the spin speed traverses the natural frequency of the suspension unit (critical frequency) cause the suspension unit to strike its supporting unit. Therefore, the most severe vibrations are produced by the centrifugal forces through the spin cycle and while traversing the critical speed. As a result of these severe vibrations, some parts of the washing machine such as the roller bearings can be damaged.

The unbalance in washing machines is to be investigated in this Chapter. These are: the effects of the unbalance on the vibration of the tub and the estimation of the unbalance amounts presented in section 3.1 and the effects of the unbalance on the motor of the washing machine discussed in section 3.2.

3.1. The Effects of the Unbalance on the Vibration of the Tub and the Estimation of the Unbalance Amount

The unbalance amount in a washing machine is detected by investigating the effects of the unbalances on the vibration of the tub especially for spin speeds over 800 rpm.

The tub of the actual washing machine has six degrees of freedom as a rigid body. To see the effect of the unbalance on the tub, one can use the simplified single degree of freedom model of the tub developed by Türkay and Taşpınar (1995). The equation of motion of the simplified single degree of freedom model is given as

$$M\ddot{x} + c_{eq}\dot{x} + k_{eq}x = F_o \sin \omega t \tag{3.1}$$

Here, M, c_{eq}, k_{eq}, F_o and ω represent the total mass of the washing unit, equivalent viscous damping coefficient, equivalent stiffness, the magnitude of the centrifugal force and the rotational speed of the drum, respectively. The magnitude of the centrifugal force caused by the unbalanced laundry is equal to

$$F_o = m_u \omega^2 \tag{3.2}$$

where m_u and ω denote the unbalance eccentricity which is equal to unbalance laundry mass times the drum radius and the drum spin speed, respectively. After substituting $x = Xe^{-i\omega t}$ into equation (3.1) and solving for x, the displacement amount subject to the unbalanced load is found as

$$X = \frac{m_u \omega^2}{k_{eq}\sqrt{\left(1 - \frac{\omega^2}{\omega_n{}^2}\right)^2 + \left(\frac{2\zeta_{eq}\omega}{\omega_n}\right)^2}} \tag{3.3}$$

The above equation is transformed into the following form by dividing both sides of the equation (3.3) by $\omega_n{}^2$ which is equal to $\frac{k_{eq}}{M}$

$$X = \frac{m_u r^2}{M\sqrt{\left(1 - r^2\right)^2 + \left(2\zeta_{eq} r\right)^2}} \tag{3.4}$$

where X and ϕ represent the steady state amplitude and phase angle, respectively. In equation (3.3), ω_n denotes the undamped natural frequency of the system. In equation (3.4)

$$\zeta_{eq} = \frac{c_{eq}}{2\sqrt{k_{eq}M}}$$

and

$$r = \frac{\omega}{\omega_n}$$

indicate the equivalent damping factor and the non-dimensional frequency, respectively. If we rearrange the equation (3.4) for the static amplitude then we obtain the following form

$$H(r) = \frac{MX}{m_u} = \frac{r^2}{\sqrt{\left(1-r^2\right)^2 + \left(2\zeta_{eq} r\right)^2}} \qquad (3.5)$$

where $H(r)$ is called the dynamic factor. Figure 3.1 indicates the plot of the dynamic factor with respect to the non-dimensional excitation frequency r.

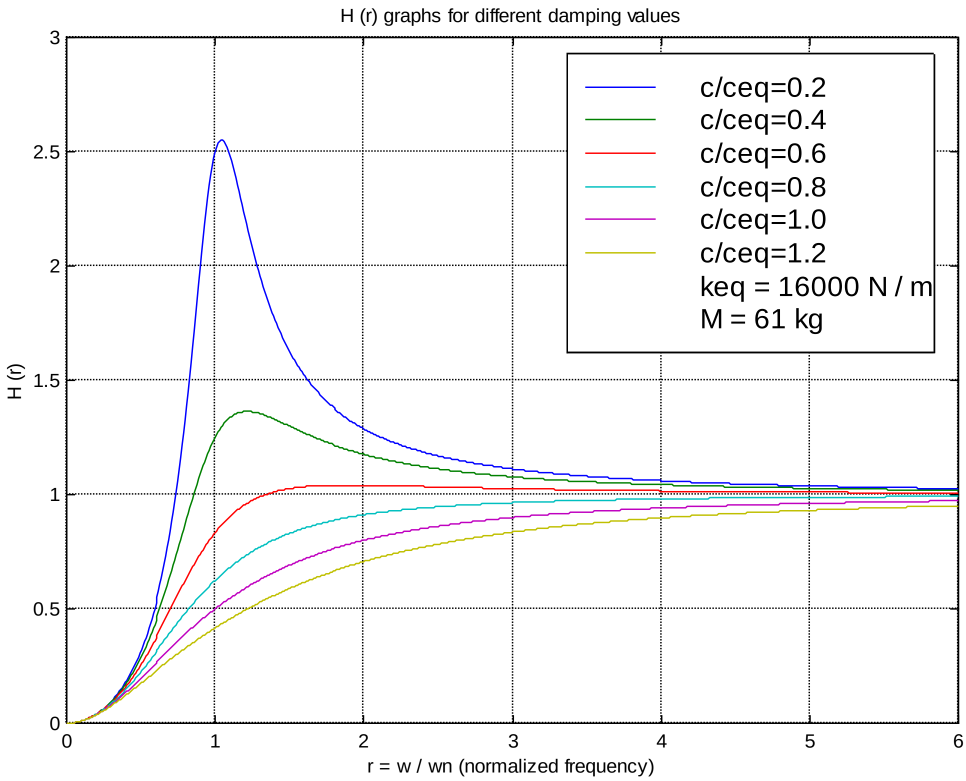

Figure 3.1. Dynamic factor versus the non-dimensional excitation frequency (r)

It is noted from Figure 3.1 that for high spin speeds the dynamic factor *H(r)* does not depend on any system parameters and goes to unity. That is, when $\omega > 800 rpm$, $H(r) = \frac{MX}{m_u}$ is equal to 1. It is seen that the unbalanced load can be estimated by measuring the vibration amplitude for high spin speeds by using the following equation

$$m_u = \frac{1}{MX} \tag{3.6}$$

3.2 The Effect of Unbalance on the Motor of the Washing Machine and its Estimation

A washing machine has three basic functions. These are: wash, rinse and spin dry. During washing only the lower one third portion of the drum is filled with water mixed with detergent, and laundry items being washed are repeatedly lifted by the paddles located on the edge of the drum. These items fall again into the water for renewed soaking, rubbing and compacting. During rinsing and spin-drying, the drum and its content are spun about the machine axis of symmetry and water is gradually drained. During the spin cycle, there is a tendency for the laundry to bunch up and gather on one side of the drum. Thus, unevenly distributed laundry in the drum causes unbalance in the rotating system. During the spin cycle, while descending downwards the potential energy of the unbalanced laundry (PE) decreases during downward motion while its kinetic energy (KE) increases. On the other hand, while ascending upwards, PE increases and hence KE decreases.

$$m_{dengesiz} g\Delta h = \frac{1}{2} m_{dengesiz} r^2 \left(\omega_{upper}^2 - \omega_{lower}^2 \right) \tag{3.9}$$

Clothes in the drumstick on the drum's wall properly after traversing the rotational speed value of *70 rpm*. This result is determined from the below equation

$$m g = m \omega^2 r \tag{3.10}$$

$$\omega = \sqrt{\frac{g}{r}} \tag{3.11}$$

where r represents the unbalance distance and g is the gravitational acceleration. Natural frequency of the washing machine suspension system corresponds to nearly *170 rpm*. It is understood that *100 rpm* is the reliable spinning cycle since *100 rpm* is well beyond the natural frequency of the system and laundry sticks at this speed on the drum wall properly.

Some assumptions are made for the estimation of the load torque produced in the system. First, the unbalanced mass is considered as a point mass. Second, the rotating system is assumed to be symmetric about its axis of rotation. At the rotational speed of *100 rpm*, it is also accepted that the unbalanced mass on the drum's wall properly. In other words, the rotating unit of the washing machine and the unbalanced mass are considered as a single system. Finally, the unbalanced mass is considered to be located at the center of the rotating axis of the drum. Following the above mentioned assumptions, the load torque produced by the unbalanced laundry can be calculated as,

$$T_L = m_{dengsiz} g r \cos(\omega t) \tag{3.12}$$

where g denotes the gravitational acceleration. It is noted from equation (3.12) that the load torque or moment is directly proportional to the unbalanced eccentricity (m_u) and harmonic function of the drum rotational speed. Moreover, the required torque that must be generated to be able to hold the reference speed at *100 rpm* is increased by the amount of $m_{dengsiz} g r \cos(\omega t)$ due to the unbalanced laundry. This condition creates fluctuations on the reference speed as to be inferred from equation (3.9). The schematic of the rotating system given in Figure 3.2 is drawn here in the light of assumption making above.

The motor moment is directly proportional to the driving current for brushless direct drive motors. As the unbalanced mass is going up and down, the needed torque from the motor changes harmonically and so does the current. Therefore, the unbalanced mass amount can be detected by examining the motor current. This requires additional sensors and an analog to digital converter card. Also, to sense the signal exactly and to refine the signal from noise, additional filters must be used. Therefore, estimation of the unbalance existing in the system is performed by manipulating the rotational speed data. The rotational speed values are gathered from the rotary

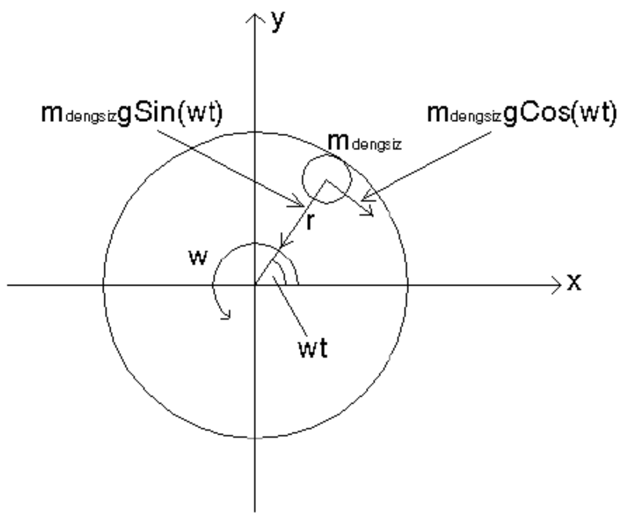

Figure 3.2 The schematic of the rotating system

encoder located on the motor. The rotary encoder produces a signal whose frequency is equivalent to the motor frequency. A closed-loop control algorithm is used to keep the rotational speed at the preset speed value of *100 rpm* so as to see the effect of unbalance on the speed. The estimation of the unbalanced load is based on the manipulation of the speed data. If the closed-loop controller does not respond quickly enough, the speed values fluctuate about the reference speed in proportion to the unbalanced load. The upper and lower bounds of speed data depend on the unbalanced load. The drum is rotated at *100 rpm* about *20 seconds* to be able to get enough data for the estimation of the unbalanced load amount. Figure 3.3 indicates a waveform created on the motor speed due to the unbalance.

After the drum reaches steady state, the speed information taken from the rotary encoder is manipulated so as to obtain meaningful information that indicates the degree of unbalance. To achieve this, the absolute value of each speed value is taken initially and then the difference from the reference speed is determined for each of the speed values. This is done for nearly *200* speed data points successively and the standard deviation is calculated as

$$std = \left[\frac{\sum_1^n \left(|\omega_i| - 100 \right)^2}{n} \right]^{\frac{1}{2}} \tag{3.13}$$

Here n has the value of *200* and ω is the motor speed in rpm. The standard deviation result corresponds to a value directly proportional to the unbalanced load amount.

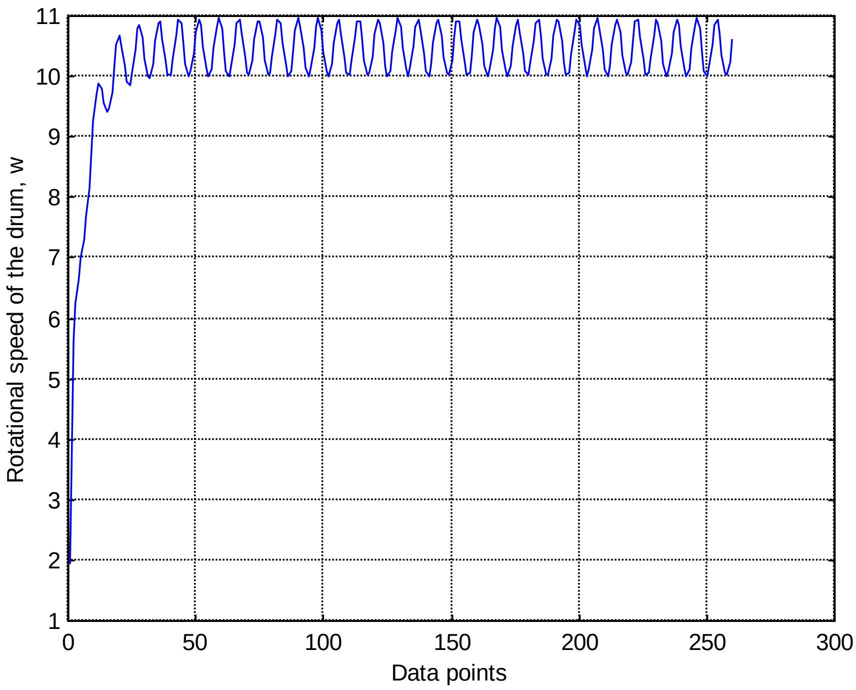

Figure 3.3 Rotational speed of the drum versus number of the data points

Figure 3.4 obtained using HP VEE data acquisition program shows the motor speed behavior for an unbalanced mass value of *800g*. The standard deviation is found to be *10.37* for this unbalanced load amount.

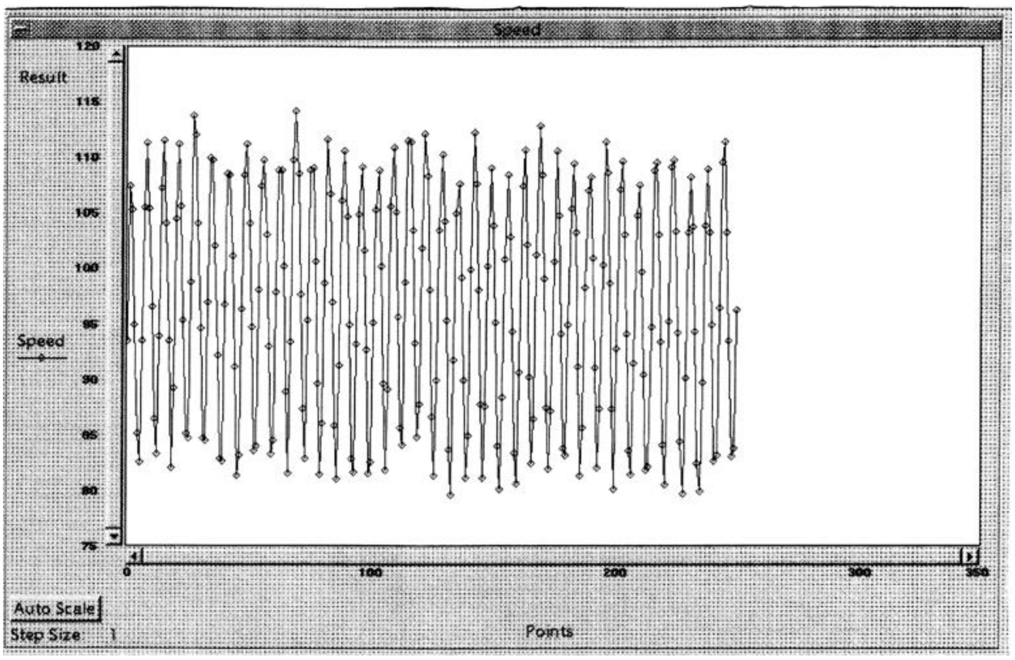

Figure 3.4 The motor speed behaviour of the washing unit at the drum speed of 100 rpm

3.3. Simulation

In this work, our aim is to form a look-up table or an inference system for each pair of balanced and unbalanced mass using dynamic model of the rotating system in order to estimate the unbalances created in the washing machine system using this look-up table. This is done by forming block diagram performing velocity control at 100 rpm using SIMULINK package of the MATLAB software program.

The standard deviation data for each combination of balanced and unbalanced mass is experimentally obtained using data acquisition hardware with HP VEE software program. Speed information coming from rotary encoder connected to the motor shaft is submitted to the PC by the DAQ hardware including HP E1332A counter card. Then, the deviation of the rotational speed values from the reference rotational speed of *100 rpm* is stored on-line to a file by employing HP VEE software program. Approximately *250* speed data points are obtained within *200 seconds* to determine the standard deviation for a balanced and unbalanced mass pair and the result is displayed on the monitor.

The block diagram of the closed-loop velocity control system is shown in Figure 3.5. This block diagram is to be investigated in four sections. These are: deriving the dynamic model of the rotating system that is to be mentioned in section 3.3.1; the calculation of the total inertia and damping existing in the rotating system that is to be talked about in section 3.3.2; the PI controller used in the closed-loop control system to hold the reference speed at 100 rpm that is to be discussed in section 3.3.3; the plots of the standard deviation graphs for each balanced mass of *0, 3, 6* and *9 kg* with the unbalanced mass increased each time *50 g* up to the *1600 g* that is to be mentioned in section 3.3.4

Simulation of the real system is made for the sampling time of *77 ms*. Thus, we compare whether simulation results match with experimentally obtained ones for each pair of balanced-unbalanced mass combination. Simulation period is taken as *160 seconds* and for each *10 sec* the unbalanced mass amount is increased by *100 g*.

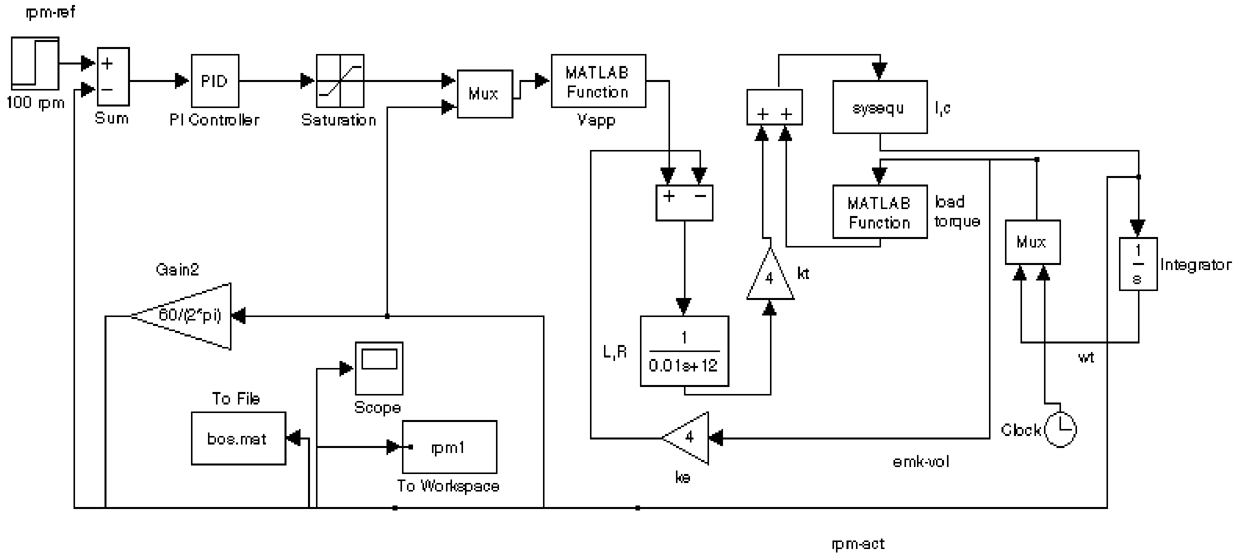

Figure 3.5. The closed-loop velocity control system

3.3.1 Modeling of the rotating system of the washing machine

The complete mathematical model of the rotating system is obtained by deriving transfer function between the motor voltage and drum rotational speed once voltage is supplied to the motor. The simulation is realized under the assumption that the rotating unit of the washing machine would be driven by a direct drive brushless DC motor. The rotor is assumed to be initially straight and torsionally rigid. The circuit diagram of the brushless direct drive motor is given in Figure 3.6 (Phillips and Harbor, 1996).

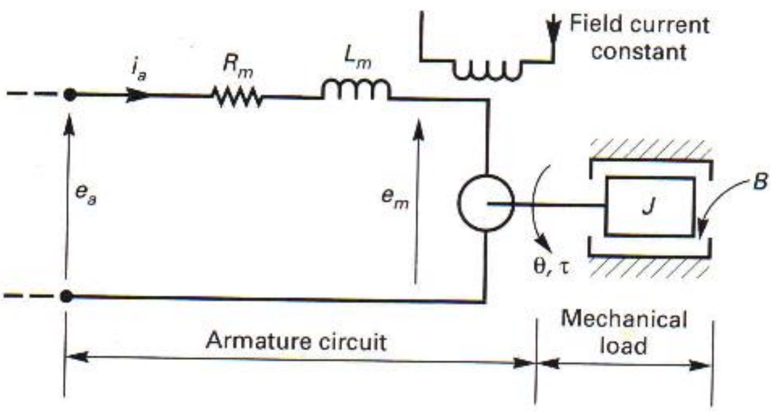

Figure 3.6. The circuit diagram of the brushless direct drive motor

In this Figure, $e_a(t)$ is the armature voltage, which is considered to be the system input. The resistance and inductance of the armature circuit are R_m and L_m, respectively. The voltage $e_m(t)$ is the voltage generated in the armature coil because of the motion of the coil in the motor's magnetic field, and is usually called the back electro motor force (EMF). The back EMF is expressed as

$$e_m(t) = K\phi \frac{d\theta}{dt} \tag{3.14}$$

where K is a motor parameter, ϕ is the field flux, and θ is the angle of the motor shaft; that is, $\frac{d\theta}{dt}$ is the angular velocity of the shaft. It is assumed that the flux ϕ remains constant; hence

$$e_m(t) = K_m \frac{d\theta}{dt} \tag{3.15}$$

The Laplace transform of equation (3.15) yields

$$E_m(s) = K_m s\theta(s) \tag{3.16}$$

For the armature circuit, we can write

$$E_a(s) = \left(L_m s + R_m\right) I_a(s) + E_m(s) \tag{3.17}$$

After solving equation (3.17) for $I_a(s)$ we obtain

$$I_a(s) = \frac{E_a(s) - E_m(s)}{L_m s + R_m} \tag{3.18}$$

The equation for the developed torque is

$$T(t) = K_1\phi i_a(t) = K_T i_a(t) \tag{3.19}$$

The Laplace transform of the above equation yields

$$T(s) = K_T I_a(s) \tag{3.20}$$

In Figure 3.6, the moment of inertia J includes the total inertia of the motor-shaft-drum assembly and the inertia of clothes, and B includes the air friction, the viscous friction in the drum and the bearing friction. Thus, the torque equation for the rotating system becomes

$$J\frac{d^2\theta}{dt^2} = T(t) - B\frac{d\theta}{dt} - T_L(t) \tag{3.21}$$

Here, T_L denotes the load torque produced by the unbalanced laundry transmitted to the motor level and is a harmonic function of the drum rotational speed.

After substituting $\omega(t)$ in place of $\frac{d\theta}{dt}$ and taking the Laplace transform of equation (3.21) we get

$$T(s) - T_L(s) = (Js + B)\omega(s) \tag{3.22}$$

Consequently, the transfer function between the effective motor torque and the drum rotational speed is obtained as

$$\frac{\omega(s)}{T(s) - T_L(s)} = \frac{1}{Js + B} \tag{3.23}$$

3.3.2 Calculation of the total inertia and damping present in the rotating system

The total inertia of the rotating system J includes the inertia of the motor-shaft-drum assembly (J_{dsm}) and the inertia of clothes. The inertia of clothes is simulated using raw rubber weights for the balanced laundry (J_{deng}) and lead weights for the unbalanced laundry $(J_{dengsiz})$. Thus, the total inertia of the rotating system is expressed as

$$J = J_{dsm} + J_{deng} + J_{dengsiz} \tag{3.24}$$

The inertia of the raw rubber weights for each balanced mass of *3*, *6* and *9 kg* is calculated using ADAMS software program. Since lead weights can be taken to be point masses, the unbalance distance r remains constant for all unbalanced mass amounts and is equal to *198 mm*. Therefore, the inertia of the unbalanced mass changing between *0* and *1600 g* is calculated as

$$J_{dengsiz} = m_{dengsiz} r^2 \tag{3.25}$$

Simulation program of the closed-loop velocity control system is run for each balanced mass amount of *0, 3, 6* and *9 kg* and for each *10 seconds* of the simulation period of *160 seconds*. At the same time, the unbalanced mass amount is raised by *100 g* until reaching the unbalanced mass amount of *1600 g*. The following figure indicates the effects of the unbalanced mass changing between *0* and *1600 g* by *100 g* on the rotational speed of the rotating unit.

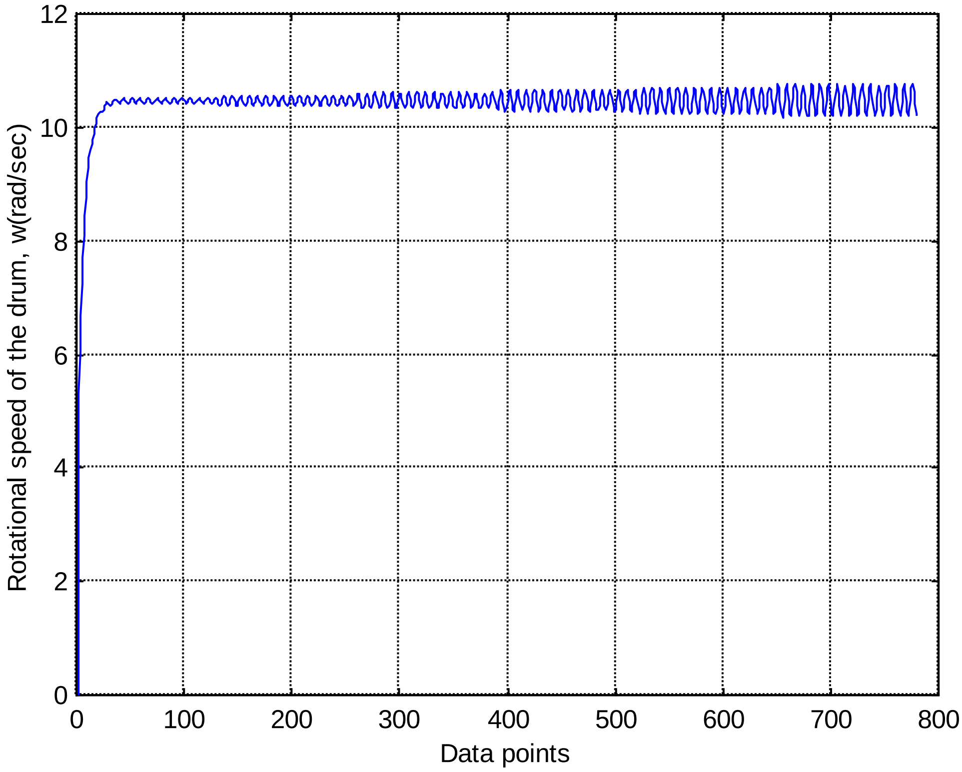

Figure 3.7. The rotational speed of the rotating unit versus the number of data points

Considering a step effective torque of magnitude T_o in equation (3.23), and solving for speed ω and taking the inverse Laplace transform results in

$$\omega(t) = T_o\left(1 - e^{\frac{-t}{\tau}}\right) \tag{3.26}$$

Here, τ is the time constant of the rotating system given by

$$\tau = \frac{J}{B} \tag{3.27}$$

τ is an indicator showing when the system reaches steady state. In general, first order systems reach steady state condition after a period of 4τ. Response speed of the system is inversely proportional to the time constant of this system; that is, a big time constant value corresponds to a slow system whereas a small time constant value corresponds to a rapid system. If we leave the washing machine rotating at ω_o freely, then the rotating unit slows down in accordance to the following equation

$$\omega(t) = \omega_o e^{\frac{-t}{\tau}} \tag{3.28}$$

After dividing both sides of the above equation by ω_o and taking its logarithm we obtain

$$\ln \omega(t) = -\frac{t}{\tau} + \ln \omega_o \tag{3.29}$$

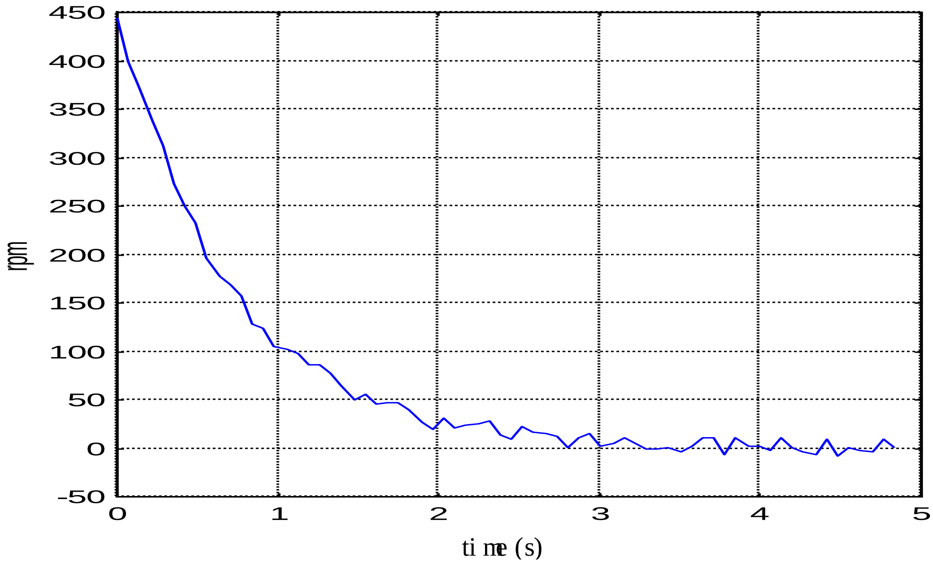

Figure 3.8 The rotational speed of the drum versus time

It is noted from equation (3.29) that the slope of the $\ln \omega(t)$ versus time graph depicted in the Figure 3.8 gives the time constant of the rotating unit and thus the damping present in the system is calculated using equation (3.27). As a result, the damping existing in the rotating system for each value of the balanced mass is calculated approximately from deceleration graphs of the rotating system. To obtain the time constant of the rotating system for each balanced mass, three experiments are made and the arithmetic mean of the results is taken. Hence, the time constant for each balanced mass of *0*, *3*, *6* and *9 kg* is acquired to be *3.2*, *5.3*, *7.6* and *10.5 sec*, respectively.

3.3.3 Closed-loop velocity control system

Closed loop velocity control is realized using PI controller. The analog PI controller output is given by

$$u(t) = K_p e(t) + K_I \int_0^t e(t)dt \qquad (3.30)$$

where $e(t) = 100 - \omega(t)$ is the controller input signal, u(t) is the controller output signal, and K_p and K_I are the PI controller gains. Response of the rotating system to the step input value of *100 rpm* is determined by adjusting the controller gain constants. K_p and K_I values yielding minimum overshoot and responding rather fast are found to be *5* and *25*, respectively. We also incorporate a saturation box into the closed-loop velocity control block diagram due to the current limitation of the motor used. The maximum current supplied to the motor is *7 A*. Since the simulations are performed at the drum rotational speed of *100 rpm* for each combination of balanced-unbalanced masses, the upper limit of the saturation box can be determined using the following equation.

$$V_{max} = i_{max} R_m + K_m \omega \qquad (3.31)$$

where V_{max} represents maximum voltage that can be supplied to the motor. Here, R_m, K_m and ω indicate the resistance of the motor armature circuit, the back electromotor force (EMF) constant and the rotational speed of the drum, respectively. After substituting $R_m = 12\ \Omega$, $i_{max} = 7\ A$, $\omega = 100\ rpm$ and $K_m = 4$ into the above equation, we obtain the maximum voltage applied to the motor as

$$\begin{aligned} V_{max} &= 7*12 + 4*100 \\ V_{max} &= 484V \end{aligned} \qquad (3.32)$$

3.3.4 Simulation results

The simulation program is run for each balanced mass and meanwhile the unbalanced mass amount is increased by *100 g* for each *10 sec* and simulation results (rotational speed values of the rotating system) are recorded to files such as 3kg.mat. Later, the standard deviation graphs for each balanced mass are plotted. Figure 3.9 indicates the standard deviation graphs obtained for each balanced mass.

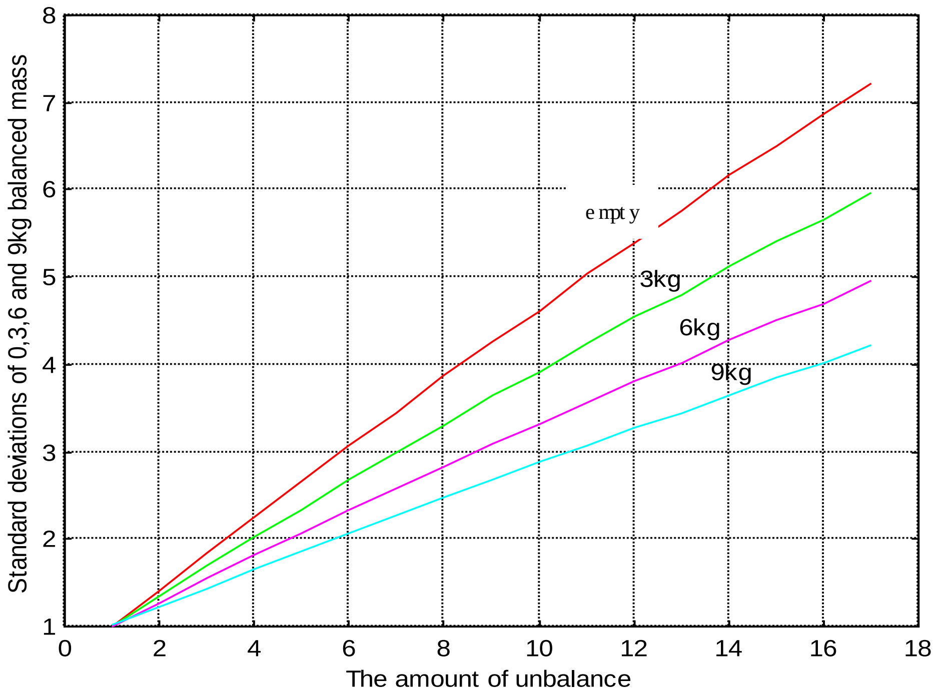

Figure 3.9. The standard deviation amount for each balanced mass versus the amount of unbalance

As expected it is seen from the Figure 3.9 that the standard deviation increases in proportion to the unbalanced mass amount. On the other hand, the standard deviation amount decreases while the balanced mass amount increases.

3.4 Measurement System and Experimental Results

Estimation of the unbalance amount in the washing machine is realized with a microprocessor based controller arrangement. Figure 3.10 illustrates a block diagram of a drum driving circuit in the washing machine.

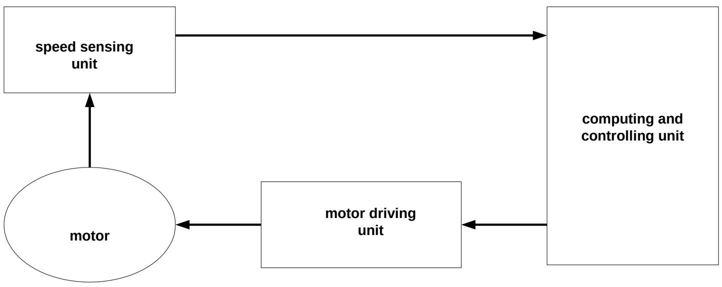

Figure 3.10. A drum driving circuit in the washing machine

The computing-controlling unit receives the rotational speed of the motor through the speed sensing unit (rotary encoder). Then, the computing-controlling unit calculates standard deviation amount at *100 rpm* and compares this value to the preset value determined beforehand. According to the comparison results, the controlling unit determines the spin profile to be followed.

The measurement setup is composed of a PC based Data Acquisition system (DAQ). In our measurement setup, we use a plug-in board to acquire data and transfer it directly to the computer. Signals coming from the rotary encoder connected to the motor are transferred to the computer by HP E1332A counter card and then by using HP VEE application software program we transform the electrical signal generated by the rotary encoder to the required rotational speed values.

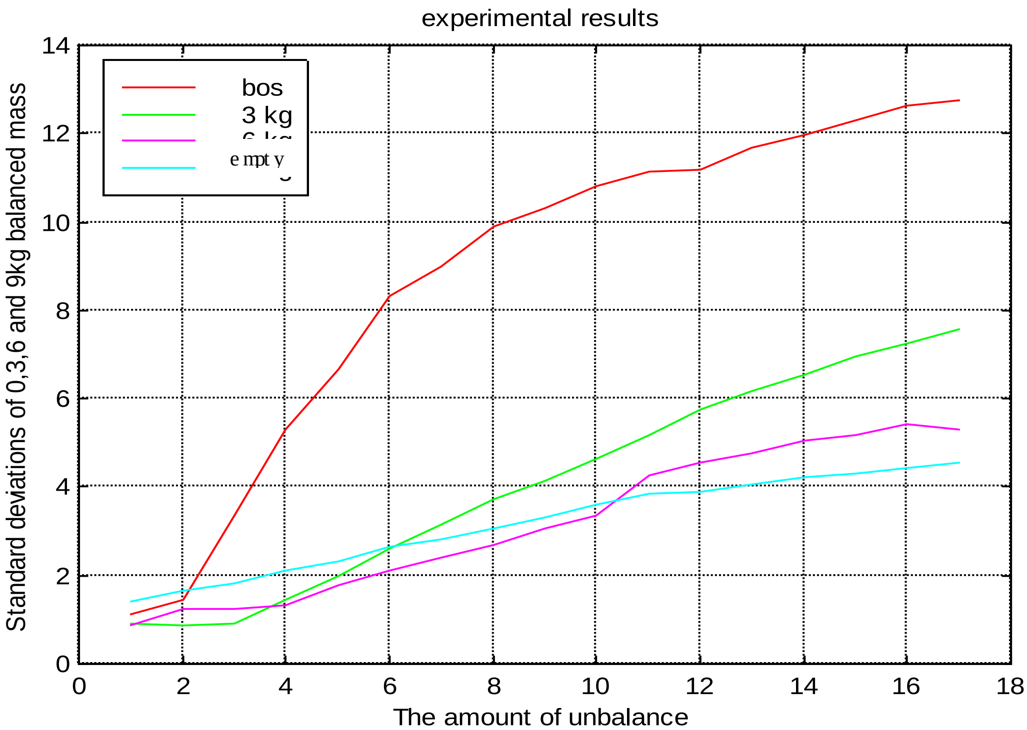

Figure 3.11. The standard deviation amount for each balanced mass versus the amount of unbalance

The controlling unit of the washing machine rotates the motor in a regular or reverse direction repeatedly at *52 rpm* until an entire washing is completed. Then, the rotational speed of the drum is increased from *52 rpm* to *100 rpm* and the rotational speed is held at this speed for a preset time period of *20 seconds* in order to acquire the needed speed data to estimate the unbalance amount existing in the system.

To obtain the standard deviation values for each balanced mass, experiments are performed with unbalanced mass increased from *0* to *1600 g* by *100 g* each time.

4. CONTROLLABLE FLUIDS AND MODEL PROPOSED FOR THESE FLUIDS

This section gives information about both controllable fluids and the devices that make use of their unique properties.

4.1. Controllable Fluids

A controllable fluid is a fluid whose rheological behavior can be externally controlled, typically by the application of either an electric or a magnetic field. The yield strength, and hence effective viscosity of these fluids can be changed by the application of the appropriate energy field. Fluids changing their viscosity and stiffness characteristics with the application of an electric field are called electrorheological (ER) fluids. On the other hand, fluids that can be controlled by the application of a magnetic field are called Bingham magnetic fluids or magnetorheological (MR) fluids. Of these two types of controllable fluids, MR fluids are currently considered to be more suitable for variable damper applications. MR fluids can provide larger yield stress, and thus are able to generate greater damping forces up to 3000N. Also, the working temperature range of MR fluids is wider and they are insensitive to contamination. Therefore, their mechanism is simpler than ER fluids that are more sensitive to contamination and thus require complex parts.

Both ER and MR fluids were initially developed in the 1940's. ER fluids were developed by Winslow as *a "method and means for translating electric impulses into mechanical forces*". MR fluids were developed by Rabinow. Initially, ER fluids received the most attention, but found to be not as well suited to most applications as the MR fluids.

In their non-activated or "*off*" state, both MR and ER fluids typically have similar viscosity, but MR fluids exhibit a much greater increase in yield strength, and therefore viscosity, than their electrorheological counter parts, as shown in Table 4.1

Table 4.1. Summary of MR and ER properties (taken from Simon, 2000)

Property	ER Fluid	MR Fluid
Yield Strength (Field)	2-5 kPa (3-5 kV/mm) field limited by breakdown (failure or ending)	50-100 kPa (150-200kA/m) field limited by saturation
Viscosity (no field)	0.2-0.3 Pa.s (at 25° C)	0.2-0.3 Pa.s (at 25° C)
Operating Temperature	+10 to +90° C (ionic to DC) -25 to +125° C (non-ionic to AC)	-40 to +150° C (limited by the carrier fluid)
Current Density	2-15 mA/cm^2 (4 kV/mm, 25° C)	can energize with permanent magnets
Specific Gravity	1-2.5	3-4
(Additional) Ancillary Materials	Any (conductive surfaces)	Iron/steel
Color	Any, opaque or transparent	Brown, black, gray, opaque

A device based on an ER fluid will have roughly the same overall power requirement as similar devices based on an MR fluid. The ER device will require high voltage, low current power, while the MR device will require low voltage, high current power. The extremely high voltage requirements for ER fluids make them impractical for most commercial applications. An additional advantage of MR fluids over ER fluids is that ER fluids are sensitive to contaminants whereas MR fluids are not. Also, MR fluids have a much broader useful temperature range than ER fluids.

4.1.1. Typical characteristics of ER fluids

An ER fluid consists of a suspension of fine semi-conducting particles in a dielectric liquid (Block and Kelly, 1988). An application of high electric field to the fluid induces a change in the rheology of dispersions and the ER fluid shows an increased resistance to flow, and in some cases conversion from fluid to solid. This increased resistance to flow is closely associated with increase of viscosity, and the rheological behavior resembles that of Bingham plastic when subjected to an electric field (Klass and Matirek, 1967). The change in fluids properties occurs within milliseconds, and is completely and immediately reversible when the electrical field is removed (H. P. Gavin, 2001). Since the voltages required to produce the required electrical fields are high, ER fluids draw very little current and it is possible to regulate several hundred kilo-Newtons of force with a few Watts.

The ER effect is primarily due to the polarization and fibration of particles that are *10* to *100* μm in diameter, suspended in dielectrically mismatched dispersant (typically a paraffin oil). The materials that can be used as the particle phase in ER suspensions are diverse and include alumina silicates, zeolites, sulfonated polymers, and carbonaceous particles. When an electric field is applied to these suspensions, the particles became polarized and interact with each other as microscopic dipoles, forming chains of particles between the electrodes. When energized, ER materials are sheared at small strains and the fibrated microstructure behaves viscoelastically.

At larger strains, the microstructure yields. At small dynamic strains, the shear stress is related to the shear strain via a complex modulus. At larger strains that are greater than roughly *0.5*, the material yields; the shear stress is in phase with the shear rate, and at intermediate strains, the material exhibits a combination of viscoelastic and yielding behavior.

Under quasisteady internal flow conditions, the shear stresses, τ, in an ER suspension are resisted by a field-dependent yielding component $\tau_y(E)$ where E represents the applied electric field and a temperature-dependent Newtonian viscous component $\eta(\theta)\dot{\gamma}$. The Bingham visco-plastic material model commonly used to model ER material under quasisteady flow is given as,

$$\tau(\dot{\gamma}, \mathrm{E}, \theta) = \tau_y(\mathrm{E})\,\mathrm{sgn}\,\dot{\gamma} + \eta(\theta)\dot{\gamma} \qquad (4.1)$$

It can be mechanically represented by a *dash-pot* parallel to a frictional element. The yield stress increases approximately with E^2, and the viscosity is roughly field independent and decreases with temperature. Stresses increase by a factor of $1+\frac{\tau_y}{(\eta\dot{\gamma})}$ when the electric field is applied. Therefore, to provide a large dynamic range, it is of importance to maintain low viscous stresses $(\eta\dot{\gamma})$. This can be accomplished by using materials with a low zero-field viscosity η and by designing devices in which the shear rates $\dot{\gamma}$ are low

Under oscillatory flow conditions, the behavior of ER materials is more complex. At small strains that is less than *0.1*, the ER material behavior is largely viscoelastic, and at larger strains that is greater than *0.5* the material follows a Bingham visco-plastic constitutive law. The transition from viscoelastic behavior to yielding behavior has been studied by several researchers for a vide variety of ER materials. D.J. Klingenberg (1993) showed that at small shear strains (10^{-4}) preyield behavior was found to follow a Kelvin viscoelastic model (D J. Klingenberg, 1993). At larger strains, the storage modulus lost its frequency dependence and decreased exponentially with increasing strain. That is, the loss modulus was found to increase monotonically with frequency over a range of strain amplitudes from 10^{-4} to 10^{1} (D J. Klingenberg, 1993). The rapid decrease in elasticity is related to disruption and reformation of the fabricated microstructure in a process responsible for the observed yield stresses in these materials. Quantitatively, these results are tightly linked to the configuration of the microstructure, but the qualitative preyield behavior was consistent among a wide set of microstructures investigated (D J. Klingenberg, 1993). Since microstructural details are not controllable in practical devices, simulation results are used to motivate a phenomenological model for the behavior of the ER vibration control device.

Numerous models have been developed to describe the behavior of MR and ER in recent years for different applications. For example, Stanway proposed an idealized mechanical model based on the Bingham viscoplastic model for the behavior of ER fluids and identified the parameters of the Bingham plastic model for an ER (Henri P. Gavin, 2001). Also, Gamota and Filisko developed a model consisting of the Bingham model (a frictional element in parallel with a dashpot) in series with a standard model of a linear solid. Spencer et. al. (1997) used a combination of springs and dashpots with a Bouc-Wen hysteretic element to model a MR damper. The

Bouc- Wen hysteresis equation is frequency independent of ER and MR materials over broad frequency ranges.

These developed models were also used in structural systems for vibration suppression. For example, Dyke et. al. (1996) has used a MR damper to experimentally control the motion of a seismically excited three story building model by using a clipped Linear Quadratic Gaussian (LQG) algorithm, and showed that by implementing the control with a MR damper, the performance could exceed that with fully active implementation. Guoguang Zhang et. al. (2000) used an ER device to suppress vibrations of industrial robots for the precise control of robot arms. Y. S. Jean et. al. (1997) used the Bingham model of ER fluids to solve vibration and noise problems due to the dynamic motion of automotive engine. Besides, S. B. Choi et. al. (1997) developed a new method for the position control of a moving table system using ER brake and ER clutch and implemented a sliding mode controller that has inherent robustness to parameter uncertainties and external disturbances.

4.1.2 Typical characteristics of MR fluids

MR fluids are the magnetic analogs of electrorheological (ER) fluids and typically consist of micron-sized magnetically polarizable particles dispersed in a carrier medium such as mineral or silicone oil. When a magnetic field is applied to the fluids, a particle chain forms, and the fluid becomes a semi-solid, exhibiting plastic behavior similar to that of ER fluids. Transition rheological equilibrium can be achieved in a few milliseconds and these fluids become devices with high bandwidth. Additionally, the achievable yield stress of modern MR fluids is in excess of *80 kPa*, allowing for devices capable of generating large forces required for full-scale installations. Moreover, The MR fluid can be readily controlled with a low voltage (e.g., $\sim 12–24\ V$), current–driven power supply producing only $\sim 1–2\ A$

4.1.3 MR damper behaviour and model chosen

Magnetorheological (MR) damper is a new semi-active control device that uses MR fluids to provide controllable dampers. A MR damper can be viewed as a regular damper whose damping properties can be changed during operation through the adjustment of the applied magnetic field. The magnetic field acts directly on the MR fluid through the activation of the coil.

Dyke, Spencer, Sain and Carlson (1997) obtained a prototype MR damper from Lord Corp. in order to evaluate the potential of an MR damper in structural control applications. The schematic of this MR damper is shown in Figure 4.1.

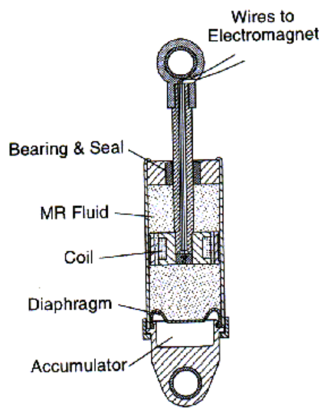

Figure 4.1 Schematic of the MR damper

The damper is *21,5 cm* long in its extended position, and the main cylinder is *3,8 cm* in diameter. The main cylinder houses the piston, the magnetic circuit, an accumulator, and 50 ml of MR fluid, and the damper has a *±2,5 cm* stroke. The total axial length of the flow channel is *15* mm, of which *7* mm are exposed to the applied magnetic field (Spencer et.al., 1997). Thus, the total volume of fluid that sees the magnetic field at any instant is about *0.3 ml*. The magnetic field can be varied from *0* to *200 kA/m* for currents of *0–1 A* in the electromagnet coil (Spencer et. al., 1997). For this system, the current for the electromagnet is provided by a linear current driver. This linear current driver generates a *0–1 A* current that is proportional to a commanded direct current input voltage in the range of *0-3 V* (Spencer et. al., 1997). Forces up to *3000 N* can be generated with this device. The rise time in the force generated by the MR damper during a constant velocity test when a step voltage is applied to the current driver is approximately *8 ms*. This behavior is primarily due to the time that the MR fluid in the damper takes to reach rheological equilibrium and the time lag associated with the dynamics of driving the electromagnet in the MR damper (Spencer et. al., 1997).

As mentioned in Chapter 2, a shock absorber having increased damping during the resonance condition (the beginning and at the end of the spin cycle) reduces the amount of the horizontally transmitted forces and thus avoids sliding of the cabinet while concurrently minimizing vibrations occurring in the suspension unit. After the drum reaches the spin speed, a shock absorber having optimum damping also decreases the amount of the horizontally transmitted forces to the cabinet of the washing unit. Carlson and David (1999) showed that incorporation of shock absorbers containing MR fluids located in horizontal axis washing machines improves their vibration suppression performance. Before using an MR damper to investigate its effectiveness in reducing vibrations caused by unbalanced laundry (washload) in horizontal axis washing machines, a realistic model of the MR damper has to be chosen.

Several mechanical models for controllable materials were developed. For example, Shames and Cozzarelli (1992) used the Bingham, viscoplastic model to describe the behavior of MR and ER fluids. In this model, the plastic viscosity is defined as the slope of the measured shear stress versus shear strain rate data for positive values of the shear strain rate, $\dot{\gamma}$, the total stress is given by

$$\tau = \tau_y(\ field\ )\, sgn(\dot{\gamma}) + \eta\dot{\gamma} \qquad (4.2)$$

where τ_y (field) represents the yield stress induced by the magnetic or electric field and η represents the viscosity of fluid.

Based on this model of the rheological behavior of ER fluids, Stanway (1987) proposed an idealized mechanical model, denoted the Bingham model, for the behavior of an ER damper. The Bingham model consists of a Coulomb friction element placed in parallel with a viscous damper and is as shown in Figure 4.2.

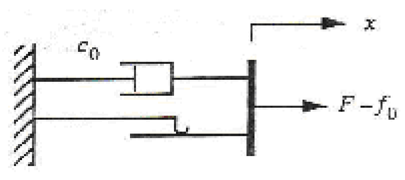

Figure 4.2 Bingham model of controllable fluid damper (Stanway, 1987)

In this model, for nonzero piston velocities, $\dot{x}$, the force generated by the device is given by

$$F = f_c\, sgn(\dot{x}) + c_o\dot{x} + f_o \qquad (4.3)$$

where

c_o : damping coefficient

f_c : frictional force related to the fluid yield stress

f_o : an offset in the force included to account for the nonzero mean observed in the measured force due to the presence of the accumulator.

The accumulator has the function of compensating for changes in the volume of the MR fluid due to changes in the temperature and changes in the volume available to the fluid as the piston rod enters and exits the body of the damper.

Also, focusing on predicting the behavior of ER materials, Gamota and Filisco (1991) proposed an extension of the Bingham model, which is given by the viscoelastic–plastic model shown in Figure 4.3.

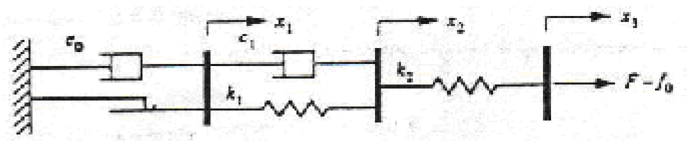

Figure 4.3. Model proposed by Gamota and Filisco (1991)

The model consists of the Bingham model (i.e., a frictional element in parallel with a dashpot) in series with a standard model of a linear solid (Shames and Gozorelli, 1992). The governing equations for this model are given by (Spencer and Dyke, 1997) as

for $|F| > f_c$

$$F = k_1(x_2 - x_1) + c_1(\dot{x}_2 - \dot{x}_1) + f_o \tag{4.4}$$

$$F = c_o\dot{x}_1 + f_c\,\mathrm{sgn}(\dot{x}_1) + f_o \tag{4.5}$$

$$F = k_2(x_3 - x_2) + f_o \tag{4.6}$$

for $|F| \le f_c$

$$F = k_1(x_2 - x_1) + c_1\dot{x}_2 + f_o \tag{4.7}$$

$$F = k_2(x_3 - x_2) + f_o \tag{4.8}$$

where c_o denotes damping coefficient associated with the Bingham model, and k_1, k_2 and c_1 are associated with the linear solid material. When $|F| \le f_c$, $\dot{x}_1 = 0$.

The other model that is numerically tractable and has been used extensively for modeling hysteretic systems is the Bouc–Wen model (Wen, 1976). This model can be used for many different purposes and can exhibit a wide variety of hysteretic behavior. A schematic of this model is shown in Figure 4.4. The force in this system is given by

$$F = c_o \dot{x} + k_o (x - x_o) + \alpha z \tag{4.9}$$

where z is an evolutionary variable governed by

$$\dot{z} = -\gamma |\dot{x}| z |z|^{n-1} - \beta \dot{x} |z|^{n} + A\dot{x} \tag{4.10}$$

By adjusting the parameters γ, β and A of the model, one can control the linearity in the unloading and the smoothness of the transition from preyield to postyield region. In addition, the force to due to the accumulator ($f_o = k_o x_o$) can be directly incorporated into this model a, an initial deflection x_o of the linear spring k_o.

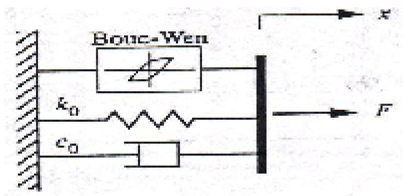

Figure 4.4 Bouc–Wen model of MR damper

The model used here is proposed mechanical model developed from the work of Spencer et al (1997) who have determined their model experimentally using a prototype MR damper (see Figure 4.1) built for control applications to better predict the damper response in the region where acceleration and velocity have opposite signs and where magnitude of the velocity is small. The schematic of this model is represented in Figure 4.5.

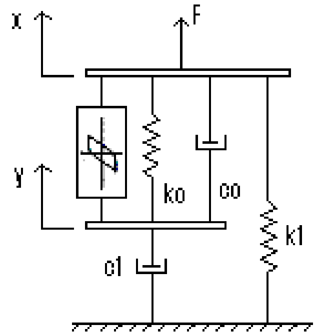

Figure 4.5. Proposed mechanical model of the MR damper.

The mechanical model of the MR damper proposed in Spencer et al (1997) is shown in Figure 4.5. A force balance on the rigid bar whose position is measured by y results in

$$c_1 \dot{y} = \alpha z + k_o(x-y) + c_o(\dot{x}-\dot{y}) \qquad (4.11)$$

where $\alpha z + k_o(x-y) + c_o(\dot{x}-\dot{y})$ represents the force generated by the Bouc-Wen model with z being called the evolutionary variable. The evolutionary variable z is calculated according to

$$\dot{z} = -\gamma|\dot{x}-\dot{y}|z|z|^{n-1} - \beta(\dot{x}-\dot{y})|z|^{n} + A(\dot{x}-\dot{y}) \qquad (4.12)$$

where γ, β, A and n denote parameters whose values are determined experimentally.

Solution of Equation (4.11) for $\dot{y}$ results in

$$\dot{y} = \frac{1}{c_1 + c_o}\left[\alpha z + c_o\dot{x} + k_o(x-y)\right] \qquad (4.13)$$

The MR damper force is then found through a force balance on the rigid bar whose position is measured by x in Figure 4.4. This force balance results in

$$F = \alpha z + c_o(\dot{x}-\dot{y}) + k_o(x-y) + k_1(x-x_o) \qquad (4.14)$$

Using Equation (4.11), Equation (4.14) can also be expressed as

$$F = c_1\dot{y} + k_1(x-x_o) \qquad (4.15)$$

In this model, k_1 represents the accumulator stiffness and c_o represents the viscous damping observed at larger velocities. The damping element represented by c_1 is included in the model to introduce the nonlinear decrease in the force–velocity relation. k_o is present to control the stiffness at large velocities and x_o is the initial displacement of spring k_1 associated with the nominal damper force due to the accumulator. By adjusting the parameters γ, β and A, the shape of the hysteresis loops for the yielding element can be controlled.

Since we need varying damping values for the washing machine suspension system over the spin cycle, we take the functional dependence of the parameters on the applied voltage (or current) into account. To account for the dependence of the parameters on the voltage applied to the current driver and the resulting magnetic current, Spencer et al (1997) suggested using

$$\alpha = \alpha(u) = \alpha_a + \alpha_b u \tag{4.16}$$

$$c_1 = c_1(u) = c_{1a} + c_{1b}(u) \tag{4.17}$$

$$c_o = c_o(u) = c_{oa} + c_{ob}(u) \tag{4.18}$$

where u is given as the output of a first order filter given by

$$\dot{u} = -\eta(u - \upsilon) \tag{4.19}$$

and υ is the commanded voltage sent to the current driver. The above equation is necessary to model the dynamics involved in reaching rheological equilibrium and in driving the electromagnet in the MR damper.

The experimentally determined parameter values of Spencer et al (1997) that are tabulated in Table 4.2 are used here.

Table 4.2 Parameters for the MR Damper model (adapted from Spencer, Dyke, Sain and Carlson, 1997)

Parameter	**Value**	**Parameter**	**Value**
c_{oa}	21.0 Ns/cm	α_a	140 N/cm
c_{ob}	3.50 Ns/cm.V	α_b	695 N/cm.V
k_o	46.9 N/cm	γ	363 cm^{-2}
c_{1a}	283 Ns/cm	β	363 cm^{-2}
c_{2b}	2.95 Ns/cm.V	A	301
k_1	5.0 N/cm	N	2
x_o	14.3 cm	η	190 sec^{-1}

Using these parameters, the response of the MR damper model is obtained for the four constant voltage levels of *0, 0.75, 1.5* and *2.25 Volts*. The inputs to the MR damper model are the displacement and the velocity across the device and the output is the force in the device. To prove the validity of the model, force versus displacement, force versus velocity and force versus time graphs were drawn and compared with those of the experimentally obtained ones of Spencer et al (1997). The simulation results are shown in Figure 4.6 and are for a displacement x (see Figure 4.5) being given by

$$x = x_o \sin(2\pi f t) \qquad (4.20)$$

The excitation frequency f has a value of *2.5 Hz* and the excitation amplitude x_o has a value of *1.5 cm*.

It is seen from these figures that the force produced by the MR damper when no voltage is applied to it is not zero. This is due to the presence of the accumulator in the MR damper. Also, the force-time plot of Figure 4.7(a) indicates that the force increases in direct proportional to the applied magnetic field. However, after a certain voltage value, this force stays at a constant value. The force-velocity hysteresis plot of Figure 4.7(b) demonstrates that the device is primarily dissipative. The hysteresis in the force-velocity plot of Figure 4.7(c) is due to the elastic and inertial properties of the material. The simulated responses obtained are in good agreement with the published experimental results (see Figure 4.6) of Spencer et al (1997).

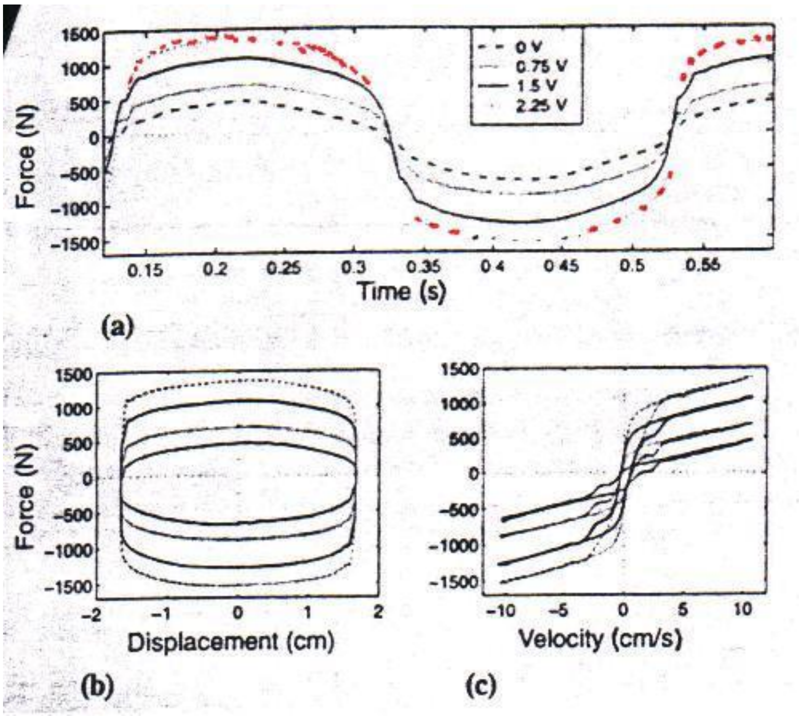

Figure 4.6 The experimental results for 2.5 Hz sinusoidal excitation with an amplitude of 1.5 cm (Spencer, Dyke, Sain and Carlson, 1997)

(a)

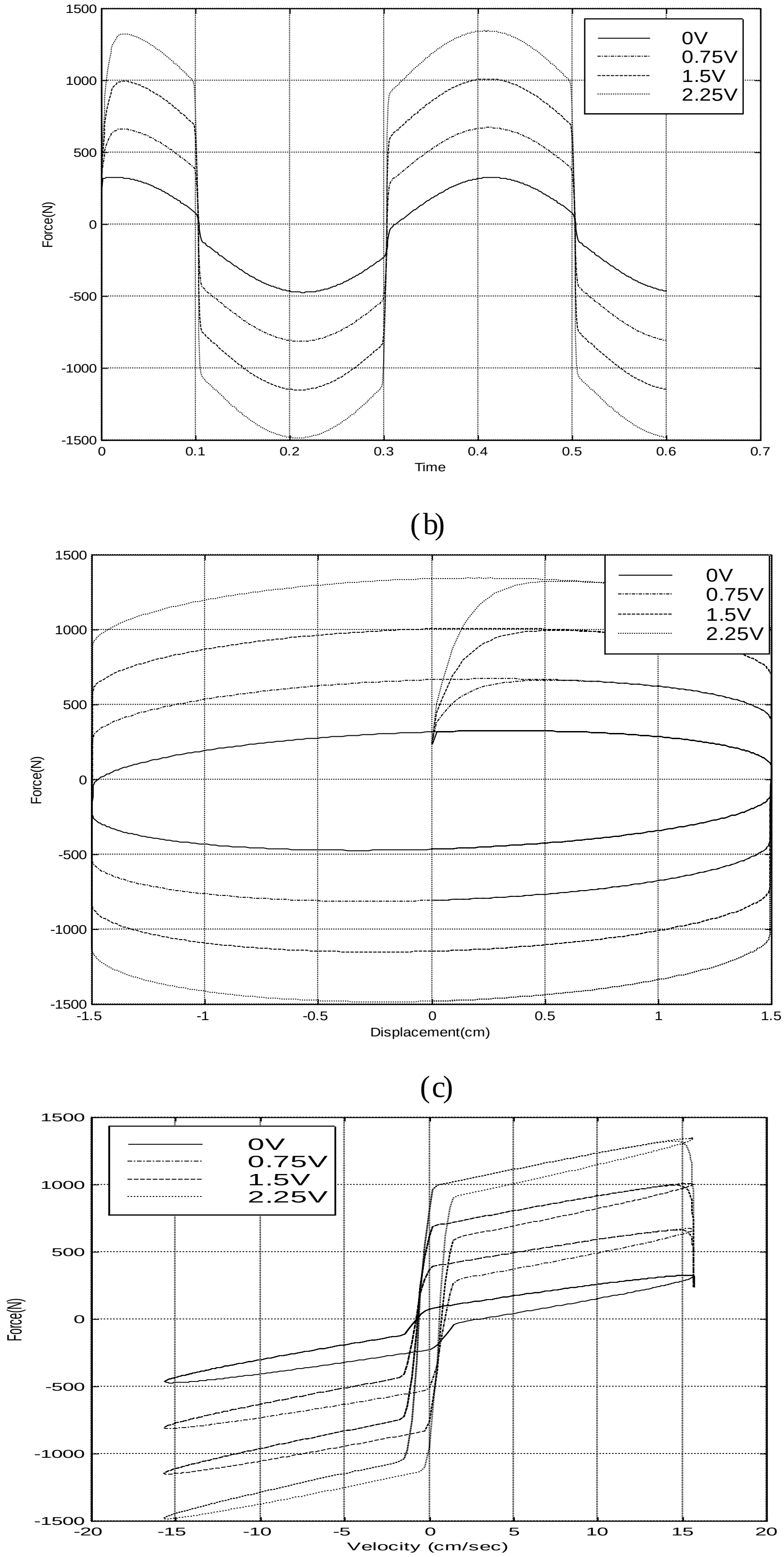

Figure 4.7. The model results for 2.5 Hz sinusoidal excitation with an amplitude of 1.5 cm.

5. ACTIVE CONTROL

The main source of vibration problems in washing machines are due to the centrifugal forces of the rotating unbalanced laundry. The magnitude of the centrifugal force depends on the location and the weight of the unbalanced laundry as well as the rotational speed of the drum. All these factors affecting the magnitude of the centrifugal forces vary during the operation of the washing machine. To damp the vibrations generated by the centrifugal forces, a friction type shock absorber ensuring a constant vibration damping capacity is being used. However, this shock absorber fails to adequately compensate vibrations whose amplitudes change during the operation of the washing machine.

Furthermore, as mentioned in Chapter 2, increased damping is needed during the resonance condition (the beginning and at the end of the spin cycle) at which vibrations and forces to be transmitted through the suspension unit reach their maximum values. On the other hand, low damping is required for minimal force transmission after the drum reaches spin speed.

The approach in vibration control for washing machine system is therefore to decrease the effect of centrifugal forces, the disturbance on the steady-state output and also on the transient response by using a controllable actuator allowing for adjusting of the damping of the washing machine system to the different washing cycles and conditions.

Before introducing the vibration control methods implemented on the washing machine suspension system to improve its washing performance, open-loop behavior of the single degree of freedom (SDOF) model of the washing machine suspension system is analyzed. In this study, the SDOF model of the washing machine system is used in order to simplify the theoretical analysis for semi-active and active vibration control. The block diagram of the open-loop passive system of the SDOF suspension model is given in Figure 5.3.

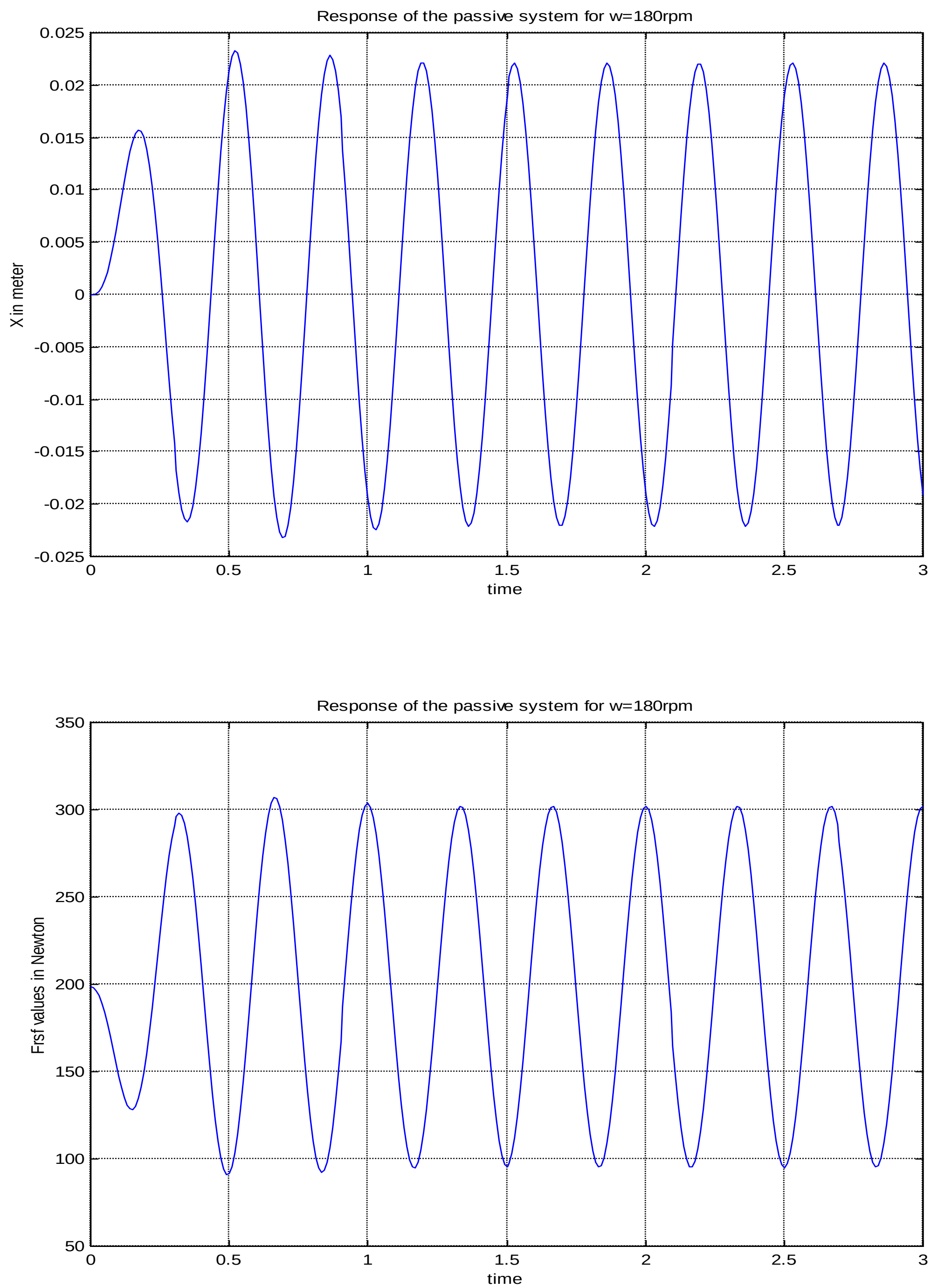

Figure 5.1. Unbalance excitation response and Frsf vs time for the drum speed of 180 rpm

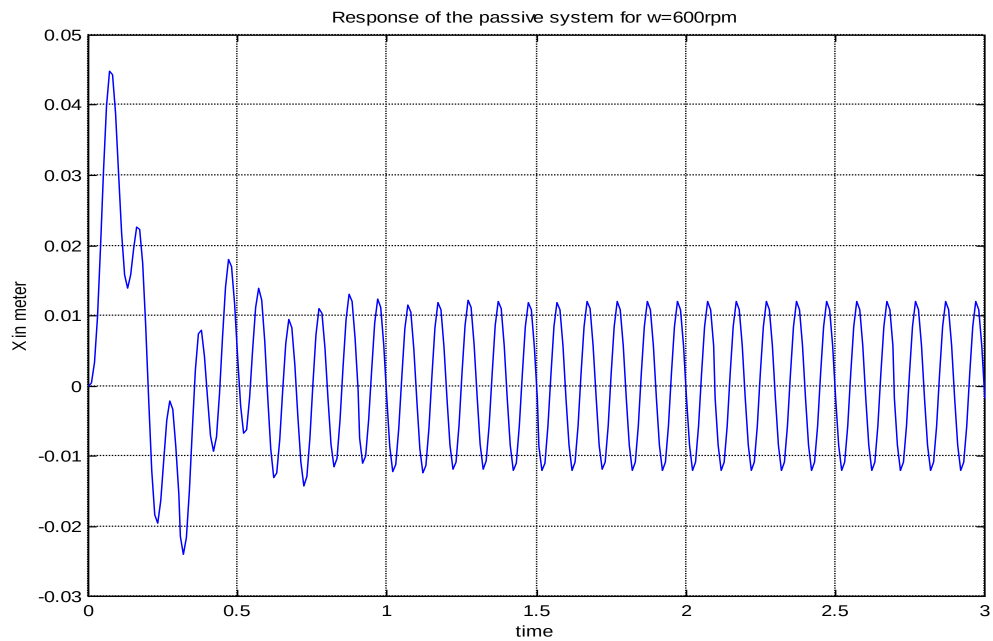

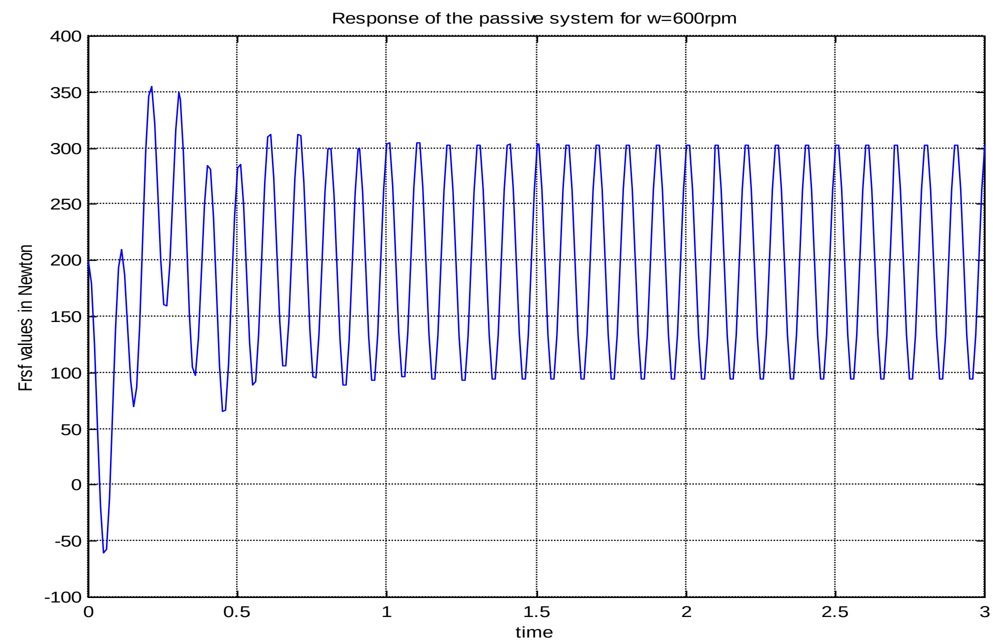

Figure 5.2 Unbalance excitation response and Frsf vs time for the drum speed of 600 rpm

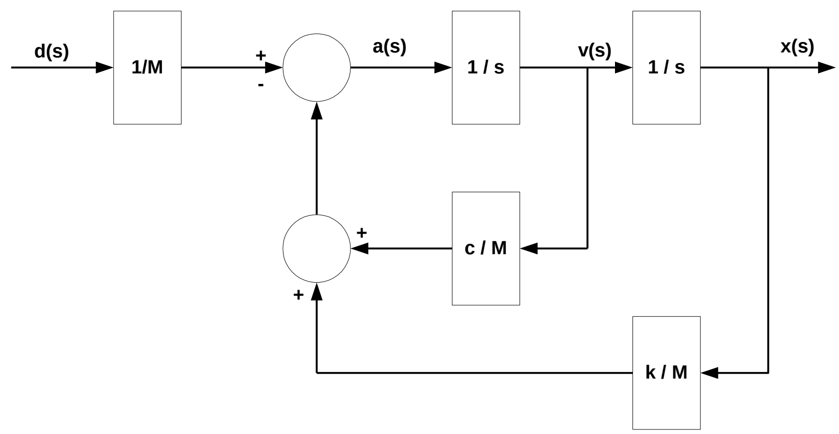

Figure 5.3. Open-loop passive system

In Figure 5.3, d(s) shows the unbalance excitation (centrifugal force) caused by the maximum unbalanced mass of *3.5 kg* rotating with the drum having a radius of *0.2 m*. The characteristics (stiffness and damping) of the optimal passive system determined by Türkay and Taşpınar (1995) are *k=16000 N/m* and *c=515 Ns/m* are used as a beginning point here. The unbalance excitation response of the passive model for two different rotational speed of the drum is given in Figures 5.1 and 5.2.

5.1. Semi-Active Vibration Control

Semi-active vibration control method relies on changing the characteristic(s) of the suspension system using a low control energy input. This control can be implemented in open-loop or closed-loop manner that is dependent upon the dynamics and the excitation of the system to be controlled. In this study, an open-loop semi-active control method is to be implemented on the SDOF model as shown in Figure 5.4.

The controllable actuator chosen here for semi-active vibration control is the magneto-rheological (MR) damper. A mechanical model of the MR damper proposed by Spencer et al (1997) is incorporated into the SDOF model of the actual washing machine in place of the dry friction shock absorber. The mechanical model proposed for the MR damper is depicted in Figure 5.5.

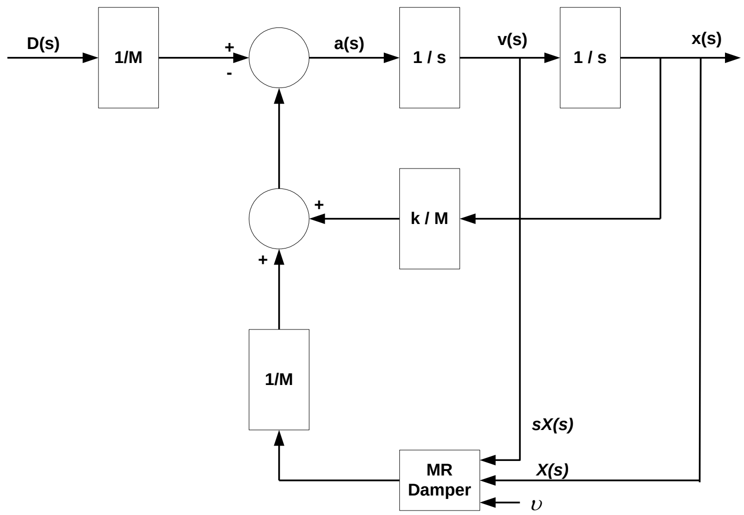

Figure 5.4 Open-loop system with the MR damper

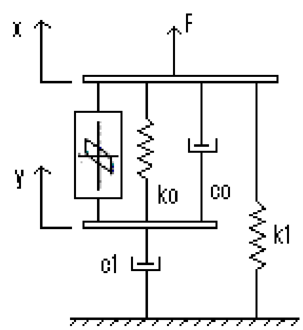

Figure 5.5 Mechanical Model of the MR damper

The damping characteristic of the MR damper is adjusted by varying the voltage υ sent to the current driver. The current driver creates a magnetic field that modifies the viscous and elastic properties of the MR medium inside the housing and thus its damping characteristics. The optimum damping of the open-loop semi-active system under the unbalance excitation for the rotational speeds of *180 rpm* and *600 rpm* is found by adjusting the voltage values applied to the MR damper to the *0.3* and *0 volt*, respectively. Figure 5.6 and 5.7 show the response of the open-loop semi-active system at these two drum speeds.

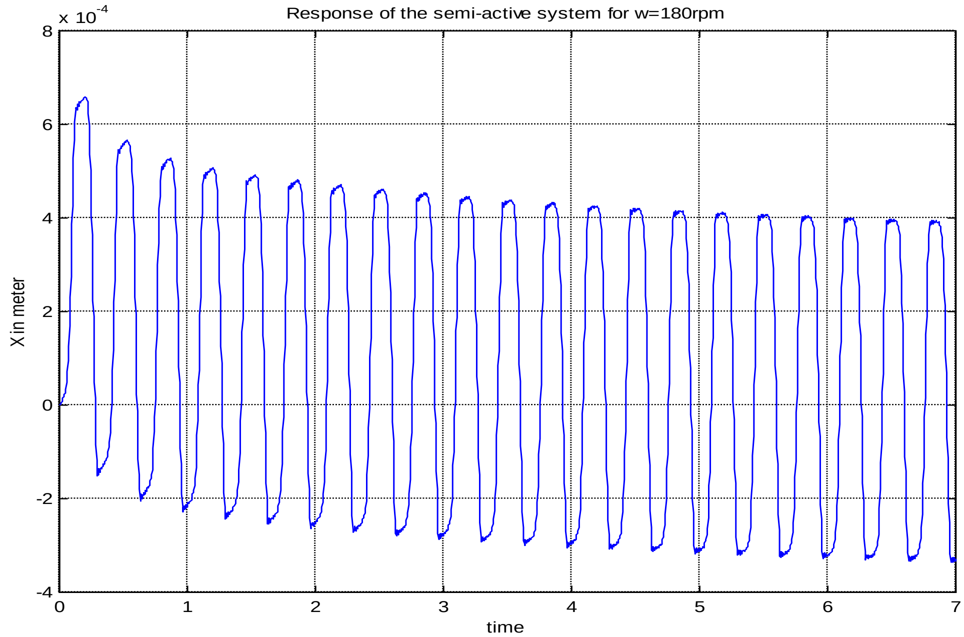

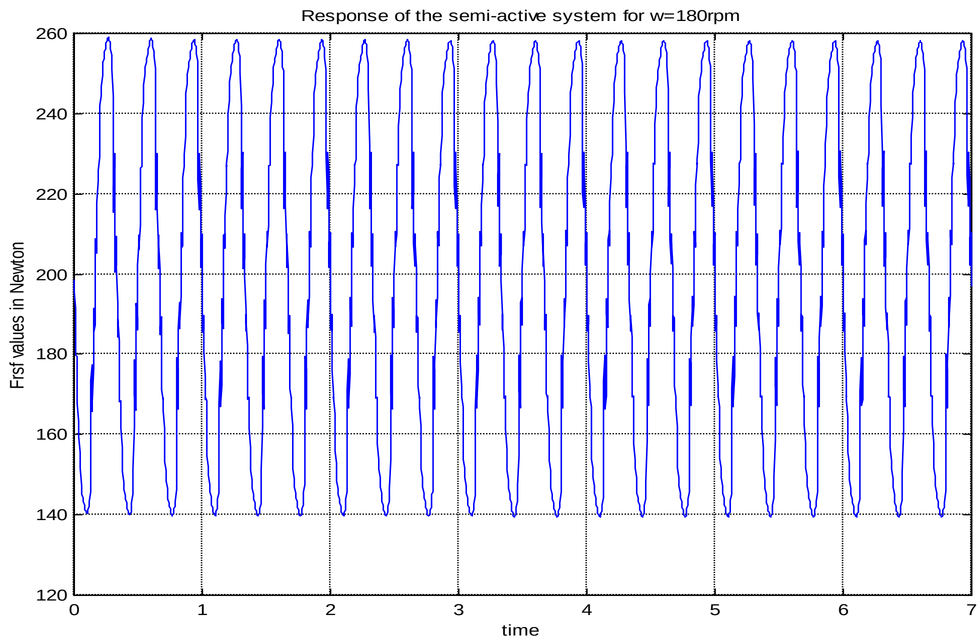

Figure 5.6. Unbalance excitation response and Frsf vs time for the drum speed of 180 rpm

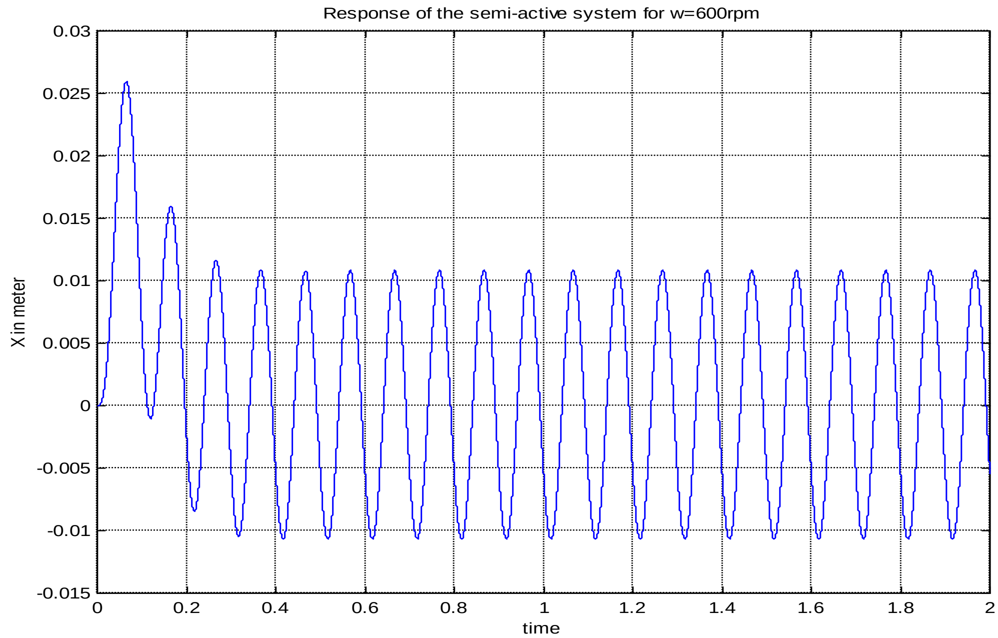

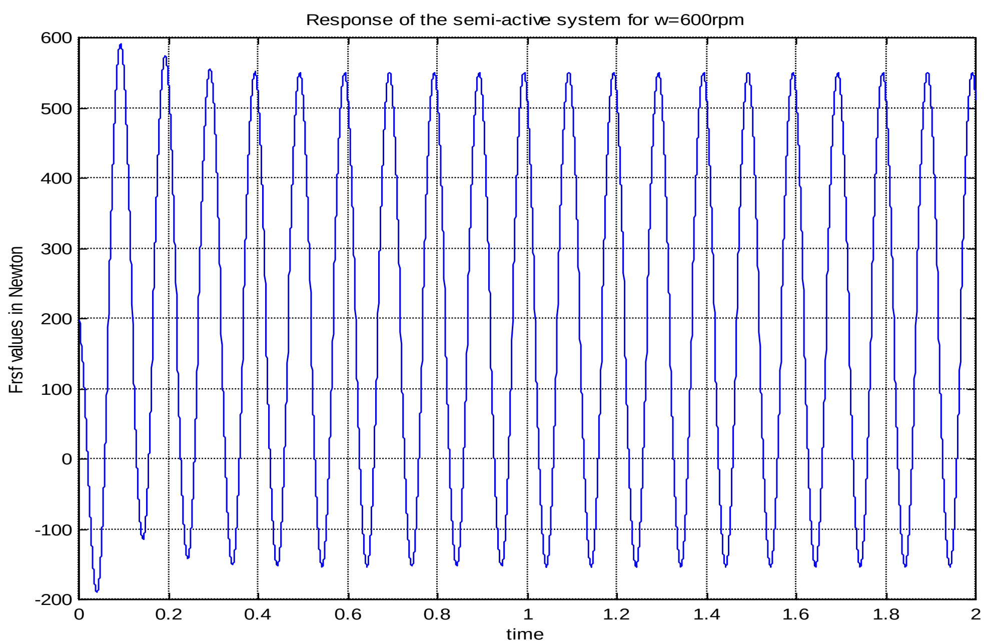

Figure 5.7. Unbalance excitation response and Frsf vs time for the drum speed of 600 rpm(MR damper shut down)

It is seen from the simulated vibration amplitude of the passive and semi-active systems that the steady state vibration amplitude of approximately *0.023 m* in Figure 5.2 has been reduced to a value of approximately *0.0004* with the MR damper as seen in Figure 5.6. A voltage of $\upsilon = 0.5$ Volt was applied in the MR damper simulation. Besides, it is deduced from comparing Figures 5.3 and 5.7 that when the MR damper is effectively shut down, its steady state vibration suppression capability is similar to that of the preferred low damping passive system.

5.2. Active Vibration Control

The first, active vibration control strategy implemented in the washing machine suspension system in this thesis is to be closed-loop control with acceleration feedback control for vibration suppression. Figure 5.8 shows the block diagram of the closed-loop system.

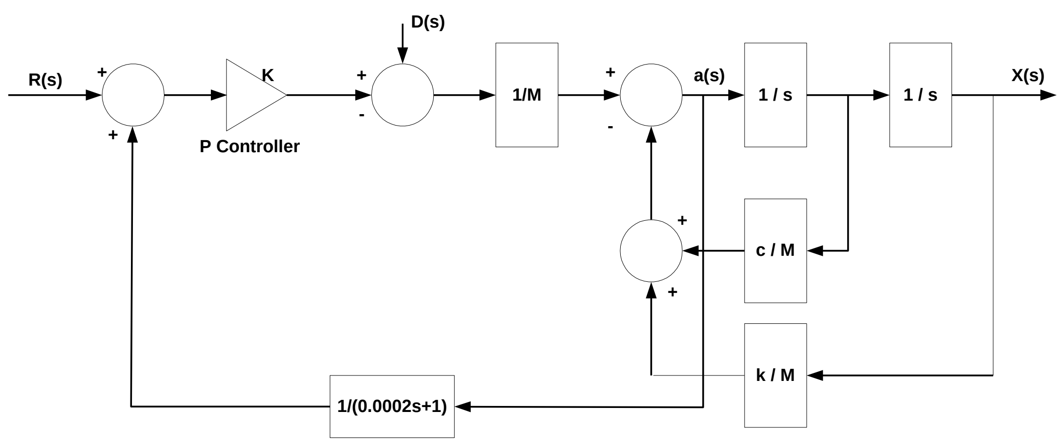

Fig. 5.8. The block diagram of the closed-loop system

In Figure 5.8 the acceleration feedback is realized by letting the control force to oppose the centrifugal forces created by the unbalanced laundry. In Figure 5.8 the accelerometer attached to the tub of the washing unit is assumed to have a transfer function in the following form;

$$H(s) = \frac{1}{\tau s + 1} \qquad (5.1)$$

where time constant, τ was chosen to have a value of *0.0002sec*. This value is sufficient to track the maximum acceleration corresponding to the maximum working speed of the washing machine system of *1500 rpm*. Note that the presence of *H(s)* in Figure 5.8 also helps prevent the formation of an algebraic loop when proportional control is used.

The proportional controller, which is essentially an amplifier with an adjustable gain is used to adjust control forces so as to attenuate vibration produced by the unbalanced laundry. The control force is drawn from the Figure 5.8 as

$$F_c(s) = Ks^2 H(s)X(s) \tag{5.2}$$

where K is the controller gain, or effective mass needed to obtain the control forces in order to suppress the disturbances generated by the centrifugal forces.

From Figure 5.8 and the above equations, the closed loop transfer functions of the washing machine suspension system from the disturbance input *D(s)* to the acceleration *a(s)* is obtained as

$$a(s) = \frac{s^2}{(K+M)s^2 + cs + k} D(s) \tag{5.3}$$

It is seen from equation (5.3) that to lower the vibration level produced by the unbalanced mass we have to decrease the effect of the disturbance. One way to achieve this is to increase the gain, K of the controller. For the predefined mass eccentricity $m_u = 0.7$ and the rotational speed $\omega = 180$ rpm the determined controller gain is found to be *170*. After simulating the system in Figure 5.8 with these values, the response of the closed-loop system is obtained.

After comparing the performance of the closed-loop system (Figure 5.9) with the open-loop passive system (Figure 5.2) it is noted that the closed-loop system reduces the vibration level for the rotational speed of 180 rpm from the value of 0.025 m to the value of 0.004 m. Thus, it is apparent that closed-loop control improves system performance. That is, the use of the acceleration feedback makes the system response partly insensitive to the disturbances.

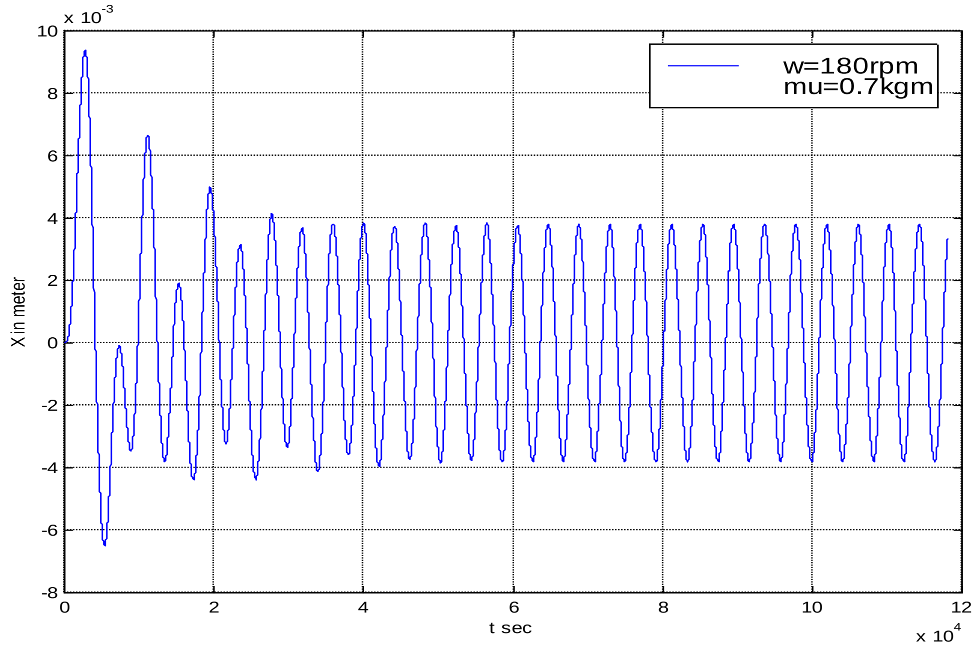

Fig. 5.9. The response of the closed-loop system with P controller

5.2.1 The application of repetitive control to the washing machine suspension system

The principle aim in this thesis is to suppress undesirable disturbances, the period of which is known since the centrifugal forces caused by the unbalanced mass is a harmonic function of the rotational speed of the drum. As repetitive control systems have been shown to work well for regulation applications involving unknown but periodic disturbance signals (Srinivasan, 1991) the repetitive controller is adapted to the washing machine vibration suppression system.

The repetitive controller contains a time delay element embedded in a positive feedback loop, the value of which is equal to the period of the periodic reference input or periodic disturbance input (Srinivasan, 1991). Since the washing machine suspension system is stable, the positive feedback loop in the repetitive controller generates the periodic signal needed at the plant input to reject the periodic disturbance signal effectively. In other words, the current control signal is based on information from the error signal measured at previous times so as to reject the periodic disturbance. Figure 5.10 demonstrates the block diagram of a single input single output repetitive control system.

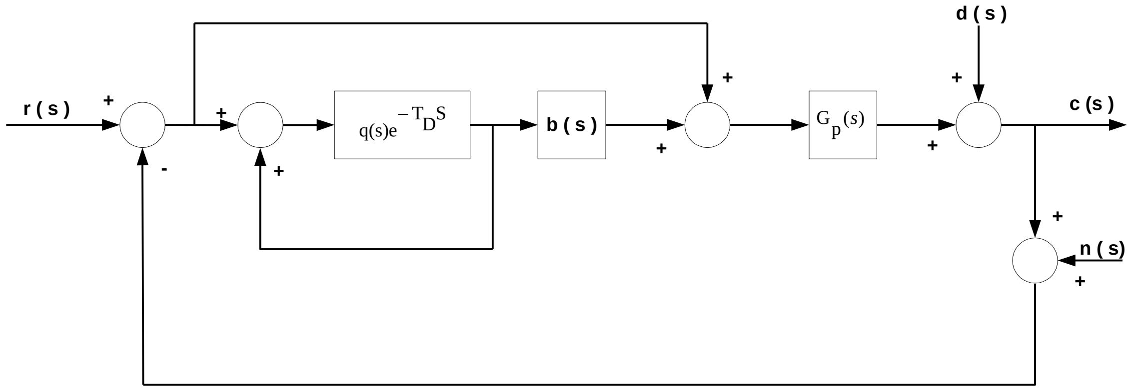

Fig. 5.10. The repetitive control system block diagram (Srinivasan, 1991)

Before introducing the repetitive controller into the block diagram of the closed-loop control system we first discuss stability analysis of time delayed systems. Srinivasan and Nachtigal (1991) developed a measure of the degree of the stability of time delayed systems. This measure is based on a function of frequency called the regeneration spectrum whose definition is based on the system characteristic equation.

5.2.2 Stability analysis of the time delayed systems using regeneration spectrum

The characteristic equation of a continuous time, time invariant, time delayed system with a single time delay T_D is given by (Srinivasan, 1991)

$$P(s)+Q(s)e^{-sT_D}=0 \qquad (5.4)$$

where *P(s)* and *Q(s)* are polynomials in the Laplace variable s. The regeneration spectrum for a time delayed system is defined as a plot of the function $R(\omega)$ given by

$$R(\omega)=\left|\frac{Q(j\omega)}{P(j\omega)}\right| \qquad (5.5)$$

versus frequency ω (Srinivasan, 1991).

The relationship of the regeneration spectrum to the absolute stability of the system is established by the amplitude phase method of stability analysis, which is essentially an application of the Nyquist criterion to time delayed systems. That is, if the polynomial *P(s)* has no zeros in the right half of the s-plane and if (Srinivasan, 1991)

$$R(\omega) < 1 \tag{5.6}$$

then the closed-loop system is stable for all values of the time delay. In other words, if the regeneration spectrum for a time delayed system is less than unity for all frequencies, the system is stable for all values of the time delay. This is a sufficient condition only and is not necessary for stability. Moreover, R is also a good measure of relative stability and it is desired to keep it as low as possible.

5.2.3 Repetitive controller design and analysis

In Figure 5.10 $G_p(s)$ is the uncompensated or conventially compensated plant transfer function, *q(s)* is a low pass filter needed to guarantee repetitive control system stability, and *b(s)* is a repetitive compensator transfer function. T_D is the period of the periodic exogenous input (Srinivasan, 1991). The characteristic equation of the closed-loop system shown in Figure 5.10 is

$$1 + G_p(s) + q(s)\left[b(s)G_p(s) - G_p(s) - 1\right]e^{-sT_D} = 0 \tag{5.7}$$

where

$$P(s) = 1 + G_p(s) \tag{5.8}$$

$$Q(s) = q(s)\left[b(s)G_p(s) - G_p(s) - 1\right] \tag{5.9}$$

Substituting *P(s)* and *Q(s)* into the equation (5.5) we get the regeneration spectrum as

$$R(\omega) = \left| \frac{q(j\omega)\left[b(j\omega)G_p(j\omega) - (1 + G_p(j\omega))\right]}{1 + G_p(j\omega)} \right| \tag{5.10}$$

$$R(\omega) = \left| q(j\omega)\left(1 - b(j\omega)\frac{G_p(j\omega)}{1+G_p(j\omega)}\right)\right| \tag{5.11}$$

The above expression for the regeneration spectrum indicates very clearly the effect of changing *q(s)* and *b(s)* on the system stability. If the equation

$$P(s) = 1 + G_p(s) = 0 \tag{5.12}$$

has no roots in the right half of the complex s-plane and if the regeneration spectrum is less than one in magnitude at all frequencies, then the repetitive control system is stable (Srinivasan, 1991). The first condition is that the closed-loop system should be stable in the absence of the repetitive control action. If compensation is required for the stability of the closed-loop system, the compensator transfer function is incorporated in $G_p(s)$. Moreover, *q(s)* and *b(s)* must be chosen in a way that an improvement in performance is to be achieved. The expression within parenthesis in equation (5.11) tends to unity as ω goes to infinity because $G_p(j\omega)$ goes to zero at high frequencies for physical systems. Therefore, $q(j\omega)$ must be lower than one at high frequencies in order to provide system stability. This is achieved by choosing a low pass filter for *q(s)*. It is also noted from equation (5.11) that choice of $b(j\omega)$ to compensate for the amplitude and phase of the frequency response $G_p/(1+G_p)$ would keep the magnitude of the term within parenthesis in equation (5.11) close to zero for a wider range of frequencies. By this way, we lower the magnitude of the regeneration spectrum, $R(\omega)$ well below unity for a wide range of frequencies and this helps improve relative stability also.

5.2.4 Application of the repetitive control algorithm to the washing machine suspension system

In this subsection, the repetitive controller is included in the block diagram of the closed-loop system so as to reject disturbances created by the unbalanced laundry.

During the spin cycle of the washing unit, there is a tendency for the laundry to bunch up and gather on one side of the drum. As a result, the concentrated laundry on one side of the drum generates centrifugal forces that are proportional to the square of the rotational speed of the drum. Since the centrifugal forces are a harmonic function of the drum rotational speed, the period of the disturbance input signal is known, which is necessary for the application of repetitive control.

The closed-loop transfer function of the washing machine suspension system has been calculated as

$$\frac{G_p(s)}{1+G_p(s)} = \frac{K_p s^2}{(K_p + M)s^2 + cs + k} \tag{5.13}$$

where $G_p(s)$ indicates the compensated plant transfer function.

Compensators *q(s)* and *b(s)* in the repetitive controller are selected using the guidelines suggested by Srinivasan and Shaw (1991). *q(s)* is chosen using the sensitivity function as a guideline for the system in Figure 5.10. The sensitivity function for the system in Figure 5.10 taken from the work of Srinivasan and Shaw (1991) is

$$S_R(s) = \left(\frac{1}{1+G_p(s)}\right)\frac{1}{1+\dfrac{q(s)e^{-sT_D}}{1-q(s)e^{-sT_D}}\dfrac{b(s)G_p(s)}{1+G_p(s)}} \tag{5.14}$$

$$S_R(s) \cong \left(\frac{1}{1+G_p(s)}\right)M_s \tag{5.15}$$

where $S_R(s)$ represents the sensitivity function for the repetitive control system.

$$S(s) = \frac{1}{1+G_p(s)} = \frac{s^2}{231s^2 + 515s + 16000} \tag{5.16}$$

where *S(s)* denotes the sensitivity function for the system without the repetitive control. *S(s)* is also termed the closed-loop transfer function from the disturbances to the outputs.

In equation (5.15), M_s demonstrates the multiplying factor changing the sensitivity function as a result of the repetitive control action (Srinivasan, 1991) and is

$$M_s(s) \cong \frac{1}{1+\frac{q(s)e^{-sT_D}}{1-q(s)e^{-sT_D}}\frac{b(s)G_p(s)}{1+G_p(s)}} \tag{5.17}$$

Since the sensitivity function, *S(s)* is used as a measure of disturbance rejection and sensitivity to plant modelling errors and parameter variation, low values of the sensitivity function magnitude $|S(j\omega)|$ are desired especially in the low frequency range. After examining the multiplying factor, M_s at low frequencies, it is seen that

$$M_s(j\omega) \cong 1-q(j\omega)e^{-j\omega T_D} \tag{5.18}$$

for the value of $b(j\omega)$

$$b(j\omega) \cong \frac{1+G_p(j\omega)}{G_p(j\omega)} \tag{5.19}$$

It is noted from equation (5.17) that the sensitivity function can be reduced to very low values for the integer values of fT_D multiplication where

$$f = \frac{\omega}{2\pi}$$

On the other hand, due to the cyclical nature of the multiplying factor, M_s the improvement in the sensitivity function is lost at the intermediate frequencies. For instance, if *q(s)* is chosen to be close to unity at low frequencies, the sensitivity function and hence error signal is reduced to nearly zero at frequencies which are integral multiples of the disturbance signal frequency, $f = \frac{1}{T_D}$ (Srinivasan and Shaw, 1991). However, at intermediate frequencies the error signal is nearly doubled.

Consequently, the eequations (5.11) and (5.17) show that improved stability require *q(s)* to be a low pass filter. Here *q(s)* is chosen as

$$q(s) = \frac{1}{0.001s+1} \tag{5.20}$$

The cut-off frequency of *q(s)* is equal to *1000 rad/sec* which is well beyond the maximum working speed of the drum of *150 rad/sec*. As proposed by Srinivasan and Shaw (1991) *b(s)* is chosen as

$$b(s) = \frac{1 + G_p(s)}{G_p(s)} = \frac{(K_p + M)s^2 + cs + k}{K_p s^2} \tag{5.21}$$

Figure 5.11 denotes the repetitive control system block diagram of the washing machine suspension system. For the drum rotational speed of *180 rpm*, T_D (the period of the disturbance input signal) is calculated as

$$f = 180 \frac{rev}{\min} \frac{1 \min}{60 \sec} = 3 \frac{rev}{\sec} \tag{5.22}$$

$$T_D = \frac{1}{f} = \frac{1}{3} \frac{\sec}{rev} \tag{5.23}$$

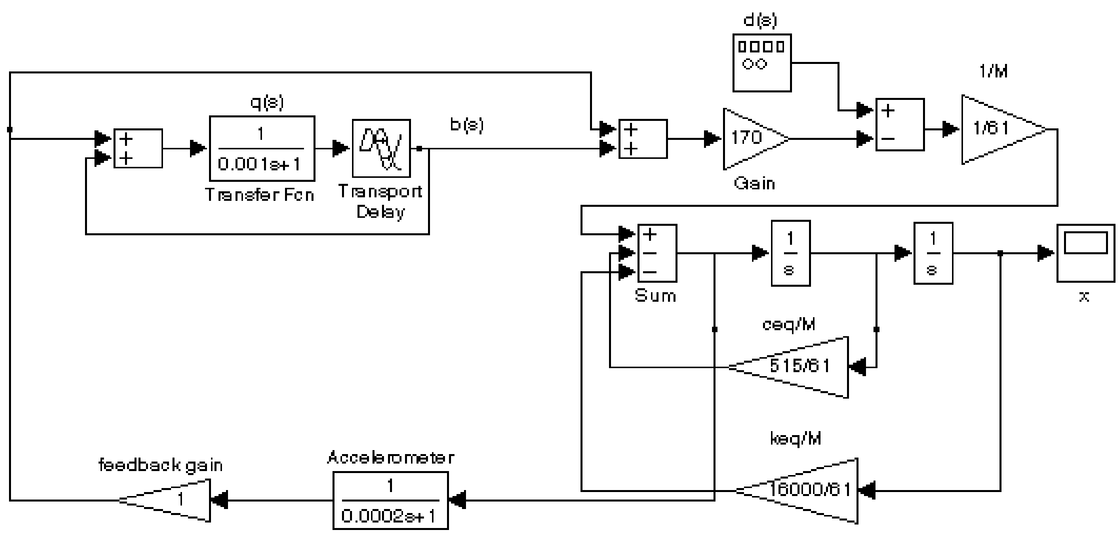

Figure 5.11. The repetitive control system block diagram of the washing machine suspension system

The response of the washing machine suspension system with the repetitive controller for the sinusoidal disturbance input signal of amplitude

$$F_o = m_u \omega^2$$

and frequency, $\omega = 180\frac{2\pi}{60}$ *rad/sec* is obtained by simulation as in Figure 5.12.

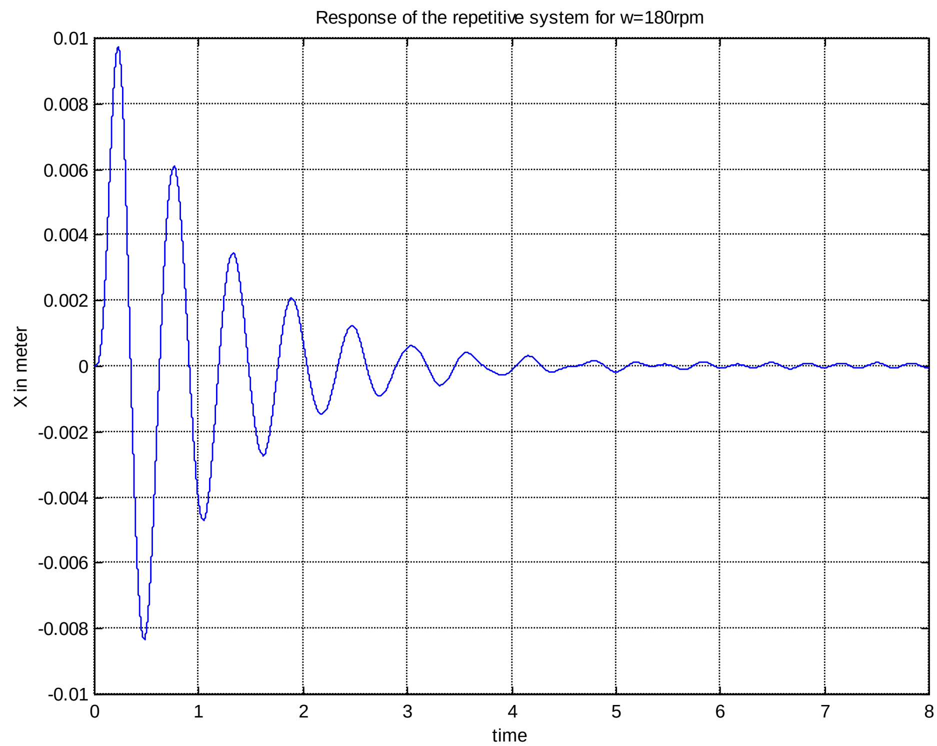

Fig. 5.12. The response of the Repetitive Control System

From Figures 5.6 and 5.12 it is noted that adding the repetitive controller into the closed-loop system the amplitude of the response is reduced approximately *100* times. That is, the amplitude of the response is decreased nearly from the value of *0.004m* to the value of *0.00007*.

Since *b(s)* is chosen to be equal to $G_p/(1+G_p)$, the regeneration spectrum goes to zero for all values of frequency. This indicates that the repetitive control system is stable for all values of frequency. The sensitivity function without and with the repetitive controller is given in Figure 5.13:

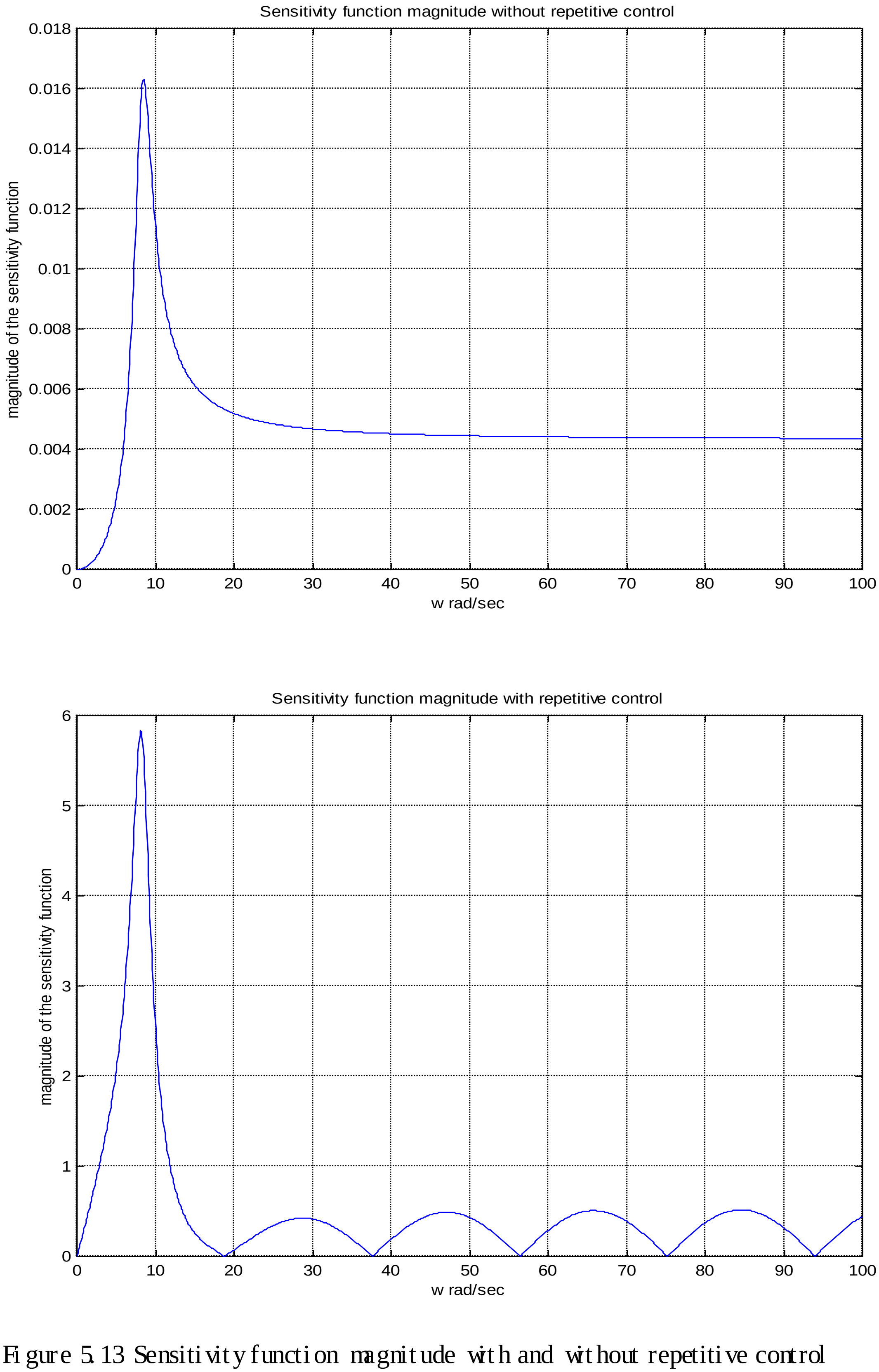

Figure 5.13 Sensitivity function magnitude with and without repetitive control

6. CONCLUSIONS AND RECOMMENDATIONS

The main source of vibration problems in washing machines are due to the centrifugal forces of the rotating unbalanced laundry. The factors affecting the magnitude of the centrifugal forces vary during the operation of the washing machine. To damp the vibrations generated by the centrifugal forces, a friction type shock absorber ensuring a constant vibration damping capacity fails to meet the required damping values which change with the rotational speed of the drum. It has been demonstrated here that the use of an MR damper allowing damping to be adjusted throughout the washing machine cycle instead of a passive damper solves this problem effectively. It is seen from the simulated vibration amplitude of the open-loop passive and semi-active control systems that the steady state vibration amplitude of the passive system has been reduced an approximately 58 times with the MR damper. Besides, active vibration control methods are applied to the passive suspension model and it is seen that the vibration amplitude of the washing machine suspension system can be suppressed completely by the application of repetitive control under ideal conditions. In addition to the effective vibration suppression performance of the MR damper, the simple mechanism, low power requirement and relatively small size of it make this controllable damper suitable in washing machine system.

To solve the walking problem of the washing machine system, it is recommended to calculate the required damping values of the MR damper off-line and to prepare a look-up table as a function of the rotating speed of the drum during the resonance condition. Then, the look-up table according to which preferred damping values are produced by the MR damper should be applied to the microprocessor of the washing machine.

REFERENCES

A. Soom and Ming-san Lee, 1983, "Optimal Design of Linear and Nonlinear Vibration Absorbers for Damped Systems", *ASME Journal of Vibration, Acoustics, Stress, and Reliability in Design*, vol. 105, pp. 112-119.

B.F. Spencer, S. J. Dyke, M. K. Sain, J. D. Carlson, 1997, "Phenomenological Model For Magnetorheological Dampers," *ASCE Journal of Engineering Mechanics*, vol. 123 (3), pp. 230-238.

B.F. Spencer, S.J. Dyke, M.K. Sain and J.D. Carlson, 1996, "Modeling and Control of Magnetorheological Dampers for Seismic Response Reduction".

C. T. Taşpınar, 1995 M. Sc. Thesis, Bogaziçi University, İstanbul, Turkey. A Semi-Active Vibration Control of a Washing Machine Suspension System.

D. C. Conrad and W. Soedel, 1995, "On the Problem of Oscillatory Walk of Automatic Washing Machines," *Journal of Sound and Vibration*, vol. 188(3), pp. 301-314.

D. E. Simon 2000 M. Sc. Thesis, Virginia Tech. University. Experimental Evaluation of Semiactive Magnetorheological Primary Suspensions for Heavy Truck Applications.

Guoguang Zhang, Junji Furusho and Masamichi Sakaguchi, 2000, "Vibration Suppression Control of Robot Arms Using a Homogeneous-Type Electrorheological Fluid", *Mechatronics, IEEE/ASME Transactions*, vol. 5(3), pp. 302-309.

G.M. Kamath, N.M. Wereley and M.R. Jolly, 1999, "Characterization of Magnetorheological Helicopter Lag Dampers" *Journal of American Helicopter Society*, vol. 44(3), pp. 234-248.

Hakan Elmali, Mark Renzulli and Nejat Olgac, 2000, "Experimental Comparison of Delayed Resonator and PD Controlled Vibration Absorbers Using Electromagnetic Actuators", *ASME Journal of Dynamic System, Measurement, and Control*, vol. 122, pp. 514-520.

Henri P. Gavin, 2001, "Control of Seismically Excited Vibration Using Electrorheological Materials and Lyapunov Methods", *IEEE Transaction on Control Systems Technology*, vol. 9, no. 1, pp. 27-36

J. D Carlson, 2000, "Washing Machine Having A Controllable Field Responsive Damper", US Pat. No: 6.151.930.

K. Srinivasan and F. R. Shaw, 1991, "Analysis and Design of Repetitive Control Systems Using the Regeneration Spectrum", *ASME Journal of Dynamic System, Measurement, and Control*, vol. 113, pp. 216-222.

K. Srinivasan and C. L. Nachtigal, 1978, "*Analysis and Design of Machine Tool Chatter Control Systems Using the Regeneration Spectrum*", ASME *Journal of Dynamic System, Measurement, and Control*, vol. 100, pp. 191-200.

L. M. Jansen and S. J. Dyke, 2000, "Semiactive Control Strategies for MR Dampers", *ASCE Journal of Engineering Mechanics*, vol. 126, No. 8, pp. 795-803.

O. S. Türkay, C. T. Taşpınar, 1995, "A Semi-Active Vibration Control of a Washing Machine Suspension System," *International Conference on Recent Advances in Mechatronics*, Istanbul, pp. 1161-1165.

P. Durazzani and L. Valent, 1999, "Method for Providing Active Damping of the Vibrations Generated by the Washing Assembly of Washing Machines and Washing Machine Implementing Said Method", US Pat. No: 5.90 "7.880.

S. B Choi, S. I. Kim and H G Lee, 1997, "Position Control of a Moving Table Using ER Clutch and ER Brake", Proceedings of the 6th International Conference on Electrorheological Fluids, Magnetorheological Suspensions and Their Applications, Yonezawa, JAPAN, July 22-25.

Y. S. Jeon, Y. T. Choi, S. B Choi and C. C Cheong, 1997, "Feedback Control for Vibration Attenuation in an ER Engine Mount", Proceedings of the 6th International Conference on Electrorheological Fluids, Magnetorheological Suspensions and Their Applications, Yonezawa, JAPAN, July 22-25.

CURRICULUM VITAE

Dilek Bayrak was born in Trabzon in 1977. She graduated from Trabzon Lycee with third ranking in 1994. In the same year, she entered Middle East Technical University, Department of Mechanical Engineering and gained her bachelor of science degree in Mechanical Engineering in 1999. In the same year, she entered the Master Program at İstanbul Technical University, Department of Mechanical Engineering, Machine Theory and Control Program. She has been working as a research assistant at İstanbul Technical University since 1999.